Epidemic modelling and control of HIV/AIDS dynamics in populations under external interactions: a worldwide challenge

Paolo Di Giamberardino[a], Daniela Iacoviello[a]

[a]*Dept. Computer, Control and Management Engineering, Sapienza University of Rome, Rome, Italy*

Abstract

In this chapter the problem of the interaction between groups of subjects singularly characterized by a specific infectious disease is addressed. The dynamical characteristics of an isolated population are preliminary studied, with particular reference to the equilibrium points and their stability. Then, the effects of constant inputs on the dynamics are deeply analysed also by numerical simulations; this analysis is propaedeutic to the study of the interaction between groups. The interactions between the different populations are modelled as additional input/output to the single group dynamics introducing total averaged effects including all the external migration effects. This approach focuses on the changes in the dynamics of one population when interactions are present without showing the global migration fluxes, but stressing the influences on each populations. Besides the simplifications of the model, this point of view may be fruitful also with respect of the design of control actions, assuming that each group can adopt the best control strategy for his own specific social characteristics. The epidemic case analysed is the HIV-AIDS one. This choice has been performed since this virus is present all over the world, but with different levels of dangerousness and number of infected patients depending on the economic, social and cultural habits. The model used is a recently introduced one, which describes this epidemic spread considering two compartments of susceptible people, distinguished by the level of attention with respect to the virus transmission, one of the infected individuals not aware of their status and two classes of patients, divided according to the level of infection. The additional inputs are introduced to model fluxes of susceptible individuals and infected not aware individuals. These effects are reported in numerous figures showing the results of numerical simulations.

Keywords: Epidemic spread, infectious disease, groups interactions, optimal control, HIV/AIDS virus, HIV model analysis.

*Corresponding author
Email address: daniela.iacoviello@uniroma1.it (Daniela Iacoviello)

2010 MSC: 00-01, 99-00

1. Introduction

In this chapter the interactions between populations affected by different diseases are discussed. In the last years, in the globalized world it has becoming more and more important to propose prompt suitable actions whenever an infectious disease starts to spread. In fact it has been estimated that, whereas in the 19th century an infectious disease took about 18 months to spread all over the world, in the recent years it takes less than 36 hours, less than the incubation period of most of the diseases. Moreover, the world population increased in the same period of about 5 times and almost 400 million of people travel every year, thus becoming possible transmission vehicles. A classical classification for epidemics refers to epidemic disease, when it is limited both from geographic and temporal point of view, pandemic disease, limited from a temporal point of view but potentially spreading in an entire continent, sporadic case, an irregular (in time and space) presence of an epidemic-like disease, endemic disease, bounded from a space point of view but not referring to a specific time. Various attempts have been made in the last years to study the spread of epidemic diseases; the main problem is to understand and to describe the modalities of the geographic spread among nations with different social characteristics and healthy weakness, as well as the effects of migration phenomena.

Being the problem so complex, in this work it is efficiently studied in sequential steps: first, a single population with a disease is analysed, along with the effects of the different control actions when acting separately; then, by using such results, the effects of changes introduced on that population when interacting with external world are deeply discussed. These interactions may be suitably modelled as additional changes in the parameters values and by introducing additional inputs as sum of the effects of migration.

The case study analysed in this chapter is the Human Immunodeficiency Virus (HIV); it is is responsible of the Acquired Immune Deficiency Syndrome (AIDS); it infects cells of the immune system, destroying or impairing their function: the immune system becomes weaker, and the person is more susceptible to infections. The AIDS is the most advanced stage of the HIV infection and can be reached in 10-15 years from the infection. It can be transmitted only by some body fluids: blood, semen, pre-seminal fluid, rectal fluid, vaginal fluid, and breast milk; the data from the World Health Organization (WHO) confirm the dangerousness of the HIV being 1.2 million the number of people died of AIDS-related illnesses worldwide in 2014 (last update); in the same period the number of people living with HIV-AIDS is about 37 million. A significant aspect is that only 54% of people with HIV is aware of the infection. Currently no vaccine exists and the treatment consists in standard antiretroviral therapy to maximally suppress the HIV virus and stop its progression; using condom and regular analysis on subjects belonging to risk-categories could help in contrasting the spread of this pandemia. The HIV/AIDS virus suitably represents

the situation at hand: a virus spreading all over the world but with different levels of dangerousness depending on the population interested; the social, economic and cultural habits may strongly vary the dynamics among the different categories of subjects. The HIV/AIDS is generally studied by considering compartmental modelling, that is dividing the population into groups homogeneous with respect to the level of disease, as it will discussed later. In general susceptible individuals and infected ones are considered, splitting each class depending on the specific characteristics to be discussed; due to the long non-symptoms period, among the infected individuals there are evidenced those that are not aware of their situation and the ones in the pre-AIDS and in the AIDS condition. Due to its dangerousness, an effective control is required to interrupt the spread, by putting together two characteristics: with wise behaviours and the fast infection detection the virus would not spread. Three possible actions are suggested by the World Health Organization; they represent different levels of prevention:

- primary prevention: it is designed for healthy people to reduce the possibility of new infections;
- secondary prevention: it is devoted to a fast identification of new infections and risk conditions to improve the percentage of subjects that become aware of their illness by regular blood tests;
- tertiary prevention: it is the medication to the aware infected subjects.

The importance of such actions is discussed in this work by analysing the effects of each control on the number of subjects in the different categories introduced and enhancing their effectiveness when the interaction among different populations is present.

This chapter is organized as follows; in Section 2 a brief review of the relevant literature is proposed, both referring to the general HIV/AIDS modeling aspects and to the spreading processing. In Section 3 the mathematical model referring to a sinle society is described, whereas in Sections 4 and 5 the model analysis is developed in absence of control and with constant inputs respectively. The interactions between populations are deeply described in Section 6, whereas the effects of migration parameters on the individuals evolutions are devloped in 7. A final discussion of the proposed results is in Section 8; some conclusions along with future work outlines are in the final Section 9.

2. Related works

When dealing with epidemic diseases, an important role is played by the development of mathematical models at different levels; for a useful description of the social implications of the infectious spread, various models, referred to different epidemic diseases like SIR, SARS, SIRC, SEIR, HIV have been introduced and analysed Chalub and Souza (2011); X.Yan and Y.Zou (2008); Casagrandi et al. (2006); Kuniya and Nakata (2012); Jr et al. (2004), and, on

the basis of such analysis, possible control strategies, such as vaccination, drug medication and quarantine are studied, Behncke (2000); Joshi (2002); Wodarz (2001); Iacoviello and Stasio (2013); Iacoviello and Liuzzi (2008a,b); Tanaka and Urabe (2014); Di Giamberardino and Iacoviello (2017a); Di Giamberardino et al. (2018); Di Giamberardino and Iacoviello (2018, 2017b). Moreover, epidemic models can be applied in different scenarios, such as biological and social networks, Dadlani et al. (2014); Kryftis et al. (2017).

The HIV/AIDS virus spread is considered in this chapter as the disease that could affect a population. Available models of HIV-AIDS infection may be divided into two main groups: the one that is focused on the dynamics at cells levels Chang and Astolfi (2009); Wodarz and Nowak (1999); Wodarz (2001); Mascio et al. (2004) and the other that deals with the dynamic of subjects interaction Naresh et al. (2009); Pinto and Rocha (2012). The first approach it is considered that in an HIV positive subject the virus infects the CD4 T-cells in the blood; when the number of these cells is below 200 in each mm^3 the HIV patient has AIDS. In Wodarz (2001) the model includes the uninfected and the infected CD4 Tcells, the concentration of helper-independent and of the helper-dependent and the concentration of the precursors. The attention is focused on the analysis of the two equilibrium points, one corresponding to the AIDS status and the other to the Long- Term nonprogressor (LTNP) one. The same model has been simplified in Chang and Astolfi (2009) introducing the effects of cytotoxic T lymphocyte, to drive the HIV patient state into the LTNP region of attraction. A double control action aming at delaying the virus progression and at boosting the immune system is proposed in Joshi (2002), whereas in Zhou et al. (2014) the idea is to reduce the number of virus particles, beyond the increase of the number of uninfected CD4 T-cells.

The second approach is the one followed in this chapter; generally four categories are introduced: the Susceptible one (S), i.e. the subjects which are not yet infected but may contract the virus, the Infected one (I) containing subjects with HIV but are not aware of the infection, the HIV subjects that are the pre-AIDS patients (P) and the AIDS patients (A). In Naresh et al. (2009), the four-classes model considers a constant inflow of HIV infected assuming birth balancing death and migration. Also natural death is introduced; from the S class a subject could go to the I or to the P class, whereas from the I class the subjects could discover to be in the pre-AIDS class (P) or in the AIDS one (A). In Nagelkerke et al. (2002), a description of a dynamic compartmental simulation model for Botswana and India considers sex behavioural compartment, high risk and low risk, to identify the best strategies for preventing the spread of HIV/AIDS. As it will be discussed in Section 3, in this work the model adopted is the one introduced in Di Giamberardino et al. (2018); two classes of non-infected subjects are introduced by splitting the S-class considering the subjects that are not aware of irresponsible acts and, therefore, could contract the virus, and the subjects representing the wise population that, suitably informed, **try to avoid** dangerous behaviours.Therefore, in the considered approach the first level of prevention corresponds to the information effort and the use of wise attitudes to avoid the non-infected subjects to acquire the HIV infection. The

interaction between populations with different diseases is an interesting topic in a globalized world and requires prompt suitable action, Dadlani et al. (2014); Tanaka and Urabe (2014); Naresh et al. (2009). In Nowzari et al. (2016) a survey about the possible approaches to face the problem of spreading processes is presented; in particular, the concepts of network and meta-population models are discussed, as well as deterministic and stochastic ones. It is also emphasised that the same kind of modelling could be efficiently applied to spreading processing regarding information propagation through social network, viral marketing and malware spreading.

A specific work about the role of population interactions and HIV/AIDS spread is Crush et al. (2005). It is evidenced the importance of a deeply understanding of the social, behavioural and economical elements in the analysis of this virus spreading in order to yield the most effective actions.

3. The single society mathematical model

The mathematical model here adopted has been introduced in Di Giamberardino et al. (2018). It considers two classes of susceptible individuals, divided according to the difference of the probability of a contagious due to different social attitudes and behaviour: the first, S_1, represents people that are not aware of unprotected sex acts and then can easily contract the virus; the second one, S_2, denotes the part of healthy population which, suitably informed, gives a great attention to the partners and to the protections; with such a classification, the first group is the main responsible for the virus propagation. In addition to the susceptible individuals, the model considers the infected subjects, I, which are the individuals which are infected but do not know their illness status. They represent the most dangerous class, since they can have sexual relationships with the unwise susceptible individuals S_1 so spreading the infection. The diagnosed patients are divided into two classes: the P and the A, the first one representing the individuals for which a HIV (pre–AIDS) condition is diagnosed, the latter containing the ones with a diagnosis of AIDS.

Using for the state variables the same names as for the classes, for a more intuitive description, the five dimensional dynamical model describing the evolution of the population in each of the classes is designed.

On the basis of the following parameters

- β regulates the interaction responsible of the infectious propagation;
- γ takes into account the fact that a wise individual in $S_2(t)$ can, accidentally, assume a incautious behaviour as the $S_1(t)$ persons;
- δ weights the natural rate of $I(t)$ subjects becoming aware of their status;
- α characterises the natural rate of transition from $P(t)$ to $A(t)$ due to the evolution of the infectious disease;
- ψ determines the effect of the test campaign on the unaware individuals $I(t)$;
- ϕ is the fraction of individuals in $I(t)$ which become, after test, classified as $P(t)$ (ϕ) or $A(t)$ ((1-ϕ));

- ε is the fraction of individuals $I(t)$ which discover to be in the pre-AIDS condition or in the AIDS one;
- d is responsible of the natural death rate, assumed the same for all the classes, while μ is the additional death factor for the individuals $A(t)$.

the model can be written as

$$\dot{S}_1(t) = Q - dS_1(t) - \frac{c\beta S_1(t)I(t)}{N_c(t)} + \gamma S_2(t) - S_1(t)u_1(t) \tag{1a}$$

$$\dot{S}_2(t) = -(\gamma + d)S_2(t) + S_1(t)u_1(t) \tag{1b}$$

$$\dot{I}(t) = \frac{c\beta S_1(t)I(t)}{N_c(t)} - (d+\delta)I(t) - \psi\frac{I(t)}{N_c(t)}u_2(t) \tag{1c}$$

$$\dot{P}(t) = \varepsilon\delta I(t) - (\alpha_1 + d)P(t) + \phi\psi\frac{I(t)}{N_c(t)}u_2(t) + P(t)u_3(t) \tag{1d}$$

$$\dot{A}(t) = (1-\varepsilon)\delta I(t) + \alpha_1 P(t) - (\alpha + d)A(t) + (1-\phi)\psi\frac{I(t)}{N_c(t)}u_2(t) - P(t)u_3(t) \tag{1e}$$

whose compact form is

$$\dot{\xi}(t) = f(\xi(t)) + g_1(\xi(t))u_1(t) + g_2(\xi(t))u_2(t) + g_3(\xi(t))u_3(t) \tag{2}$$

once $\xi(t) = \begin{pmatrix} S_1(t) & S_2(t) & I(t) & P(t) & A(t) \end{pmatrix}^T$ denotes the five dimensional state vector of (1), and the vector fields have the expressions

$$\begin{aligned} f(\cdot) &= \begin{pmatrix} Q - dS_1(t) - \frac{c\beta S_1(t)I(t)}{N_c(t)} + \gamma S_2(t) \\ -(\gamma+d)S_2(t) \\ \frac{c\beta S_1(t)I(t)}{N_c(t)} - (d+\delta)I(t) \\ \varepsilon\delta I(t) - (\alpha_1 + d)P(t) \\ (1-\varepsilon)\delta I(t) + \alpha_1 P(t) - (\alpha + d)A(t) \end{pmatrix}, \quad g_1(\cdot) = \begin{pmatrix} -S_1(t) \\ S_1(t) \\ 0 \\ 0 \\ 0 \end{pmatrix} \\ g_2(\cdot) &= \begin{pmatrix} 0 \\ 0 \\ -\psi\frac{I(t)}{N_c(t)} \\ \phi\psi\frac{I(t)}{N_c(t)} \\ (1-\phi)\psi\frac{I(t)}{N_c(t)} \end{pmatrix}, \qquad g_3(\cdot) = \begin{pmatrix} 0 \\ 0 \\ 0 \\ P(t) \\ -P(t) \end{pmatrix} \end{aligned} \tag{3}$$

More in details, the interactions between the classes in the model (1) are given by the following terms:

i. $\gamma S_2(t)$, representing the fraction of the wise uninfected individuals that accidentally or occasionally, behaves like the unwise ones, so moving from S_2 to S_1;
ii. $S_1(t)u_1(t)$, which models the fact that, under a suitable informative campaign whose strength is given by $u_1(t)$, a proportional part of S_1 becomes wise and then moves to the S_2 class;

iii. $\frac{c\beta S_1(t)I(t)}{N_c(t)}$, modelling the interaction between the unwise people S_1 and the infected individuals which are not conscious of their condition. The term is normalised with respect to $N_c(t) = S_1(t)+S_2(t)+I(t)$, the total population that can have sexual relationships: People that become infected goes from S_1 to I, until the infection will be diagnosed;

iv. δI, the fraction of unconscious infected that discovers to be ill, some of them, $\varepsilon\delta I$, with HIV (pre–AIDS) infection, the remaining part, (1-ε)δI, positive to the AIDS;

v. $\psi\frac{I(t)}{N_c(t)}u_2(t)$, proportional to the blood analysis campaign $u_2(t)$ operated on the potentially infected $N_c(t)$, for which a positive response is given for the actual $I(t)$ subjects; as for the previous term, the results can prove a HIV infection, $\phi\psi\frac{I(t)}{N_c(t)}u_2(t)$, or an AIDS one, $(1-\phi)\psi\frac{I(t)}{N_c(t)}u_2(t)$;

vi. $\alpha_1 P(t)$ and $P(t)u_3(t)$; they describe the natural degeneration of the illness from HIV to AIDS (first term) and a therapy action to prevent such transition (second term);

vii. a natural death rate d is added to all the classes; an additional rate α is introduced for the AIDS infected individuals to consider the increased probability to die in such a critical conditions.

The external actions, which for the isolated group correspond to control inputs for the dynamical model, are defined by u_1, the informative actions to prevent dangerous relationships, u_2, the blood analysis to discover infected individuals, and u_3, the therapy action for the diagnosed patients.

A deeper explanation of the meaning and the role of each coefficient and each term, along with the motivation of their introduction, can be found in Di Giamberardino et al. (2018).

4. Stability analysis

Before starting with the analysis of the behaviour of the dynamics (1) under additional external immigration and emigration, some considerations on the equilibrium conditions and the stability for the isolated systems are briefly recalled to better understand the system behaviour.

The internal stability analysis is performed on the uncontrolled system (1), with $u_1(t) = u_2(t) = u_3(t) = 0$. First, the equilibrium points are computed and then the local stability is studied.

4.1. Equilibrium points

The equilibrium points of dynamics (1) are computed solving the non linear system

$$f(S_1^e, S_2^e, I^e, P^e, A^e) = 0 \tag{4}$$

with $f(\cdot)$ in (3) (Di Giamberardino et al., 2018). Computations give the two solutions

$$\xi_1^e = \begin{pmatrix} \frac{1}{d} \\ 0 \\ 0 \\ 0 \\ 0 \end{pmatrix} Q, \qquad \xi_2^e = \begin{pmatrix} \frac{1}{c\beta-\delta} \\ 0 \\ \frac{c\beta-(d+\delta)}{(d+\delta)(c\beta-\delta)} \\ \frac{\varepsilon\delta[c\beta-(d+\delta)]}{(\alpha_1+d)(d+\delta)(c\beta-\delta)} \\ \frac{\delta[c\beta-(d+\delta)][(1-\varepsilon)d+\alpha_1]}{(\alpha_1+d)(\alpha+d)(d+\delta)(c\beta-\delta)} \end{pmatrix} Q \tag{5}$$

ξ_1^e is always a solution, while the existence of ξ_2^e depends on the fulfilment of the condition

$$c\beta - (d+\delta) > 0 \tag{6}$$

which is necessary and sufficient for the non negativeness of the equilibrium values in ξ_2^e (Di Giamberardino et al. (2018)).

4.2. Stabilty analysis

Local stability of the equilibrium points is studied making use of the linear approximations in a neighbourhood of the equilibrium point ξ_1^e and, if it exists, ξ_2^e in (5). The Jacobian matrix $J_f(\xi) = \frac{\partial f}{\partial \xi}$ must be computed and then evaluated et each equilibrium point. For the equilibrium point ξ_1^e, one gets

$$A_1 = \left.\frac{\partial f}{\partial \xi}\right|_{\xi=\xi_1^e} = \left(\begin{array}{ccc|cc} -d & \gamma & -c\beta & 0 & 0 \\ 0 & -(\gamma+d) & 0 & 0 & 0 \\ 0 & 0 & c\beta-(\delta+d) & 0 & 0 \\ \hline 0 & 0 & \varepsilon\delta & -(\alpha_1+d) & 0 \\ 0 & 0 & (1-\varepsilon)\delta & \alpha_1 & -(\alpha+d) \end{array}\right) \tag{7}$$

The block triangular structure allows to find easily its eigenvalues

$$\lambda_1 = -d,\ \lambda_2 = -(\gamma+d),\ \lambda_3 = c\beta-(d+\delta),\ \lambda_4 = -(\alpha_1+d),\ \lambda_5 = -(\alpha+d) \tag{8}$$

and the equilibrium point ξ_1^e is locally asymptotically stable if and only if

$$c\beta - (d+\delta) < 0 \tag{9}$$

As far as the second equilibrium point ξ_2^e in (5) is concerned, the block triangular structure of the linear approximating dynamical matrix

$$A_2 = \left.\frac{\partial f}{\partial \xi}\right|_{\xi=\xi_2^e} = \begin{pmatrix} A_2^{11} & 0 \\ A_2^{21} & A_2^{22} \end{pmatrix} \tag{10}$$

simplifies the analysis, since the eigenvalues of matrix A_2, denoted by $\sigma(A_2)$, are given by $\sigma(A_2) = \sigma(A_2^{11}) \cup \sigma(A_2^{22})$. Then, once the two matrices

$$A_2^{11} = \left.\begin{pmatrix} -d - \frac{c\beta I^e}{N_c^e} + \frac{c\beta S_1^e I^e}{(N_c^e)^2} & \gamma + \frac{c\beta S_1^e I^e}{(N_c^e)^2} & -\frac{c\beta S_1^e}{N_c^e} + \frac{c\beta S_1^e I^e}{(N_c^e)^2} \\ 0 & -(\gamma+d) & 0 \\ \frac{c\beta I^e}{N_c^e} - \frac{c\beta S_1^e I^e}{(N_c^e)^2} & -\frac{c\beta S_1^e I^e}{(N_c^e)^2} & -(d+\delta) + \frac{c\beta S_1^e}{N_c^e} - \frac{c\beta S_1^e I^e}{(N_c^e)^2} \end{pmatrix}\right|_{\xi=\xi_2^e} \tag{11}$$

and

$$A_2^{22} = \begin{pmatrix} -(\alpha_1 + d) & 0 \\ \alpha_1 & -(\alpha + d) \end{pmatrix} \tag{12}$$

are computed, the stability of the equilibrium point results from the stability of dynamical matrix (11), being the eigenvalues of (12), $\lambda_4 = -(\alpha_1 + d)$ and $\lambda_5 = -(a + d)$, always negative.

The eigenvalues of (11) can be computed solving the equation

$$\lambda^2 + (c\beta - \delta)\,\lambda + \frac{(d+\delta)(c\beta - (d+\delta))(c\beta - \delta)}{c\beta} = 0 \tag{13}$$

since $\lambda_3 = -(\gamma + d)$ is straightforwardly obtained.

For the Descartes' rule of signs, the equilibrium point is locally asymptotically stable if

$$c\beta - (d + \delta) > 0 \tag{14}$$

This means that the equilibrium point ξ_2^e is locally asymptotically stable if and only if (14) holds. Therefore, it is possible to conclude that if ξ_1^e is the only equilibrium point ((9) satisfied), it is also locally asymptotically stable. If the second point ξ_2^e exists, then ξ_1^e results to be unstable while ξ_1^e is locally asymptotically stable.

Such a behaviour depends on the values of parameters $c\beta$, d and δ. On the basis of their meanings, the existence and the stability of the two different equilibrium points depend on the relative values of probability of the infection transmission ($c\beta$) and the velocity of reduction of the infected $I(t)$ by natural death (d) or by infection diagnosis (δ).

5. Equilibria and stability analysis under constant inputs

In this Section, the effects of the presence of constant inputs on the existence of equilibrium conditions for dynamics (1) and the corresponding stability properties are studied. The aim is to compute where the new equilibria are located and if the stability properties are changed or not, in order to investigate the effects of the inputs in view of the addition of possible external input arising from the interaction between groups.

This analysis is motivated observing that interactions with other groups can be also represented by suitable inputs (migrations, travels, daily movements cross the borders etc.). Then, preliminary, the inner controls u_1 and u_2 are introduced and their effects are studied. For sake of clarity, in order to put in evidence the contribution and the effects of each control input introduced, the study is performed analysing the dynamics under the action of one input at a time.

5.1. Analysis of the case $u_1(t) = u_1 =$const, $u_2(t) = u_3(t) = 0$

The study of the changes in the equilibrium points and their stability conditions under the hypothesis that the control u_1 assumes a constant value different

from zero is here performed. First, the equilibria are computed and the relationships with the uncontrolled equilibria are investigated. Then, their stability conditions are checked.

5.1.1. Computation of the equilibrium points for $u_1 \neq 0$

In this case, the system to be solved is

$$f(S_1^e, S_2^e, I^e, P^e, A^e) + g_1(S_1^e, S_2^e, I^e, P^e, A^e)u_1 = 0 \tag{15}$$

the same as (4), with the addition of $g_1(\xi(t))u_1$, with g_1 as in (3).

The solutions can be computed analytically. After some manipulations, one gets the two equilibrium points

$$\xi_1^e(u_1) = \begin{pmatrix} \frac{1}{d\left(1+\frac{u_1}{\gamma+d}\right)} & \frac{\frac{u_1}{\gamma+d}}{d\left(1+\frac{u_1}{\gamma+d}\right)} & 0 & 0 & 0 \end{pmatrix}^T Q \tag{16}$$

and

$$\xi_2^e(u_1) = \begin{pmatrix} \frac{1}{c\beta-\delta\left(1+\frac{u_1}{\gamma+d}\right)} \\ \frac{\frac{u_1}{\gamma+d}}{c\beta-\delta\left(1+\frac{u_1}{\gamma+d}\right)} \\ \frac{1}{d+\delta}\left(1-\frac{d\left(1+\frac{u_1}{\gamma+d}\right)}{c\beta-\delta\left(1+\frac{u_1}{\gamma+d}\right)}\right) \\ \frac{\varepsilon\delta}{(\alpha_1+d)(d+\delta)}\left(1-\frac{d\left(1+\frac{u_1}{\gamma+d}\right)}{c\beta-\delta\left(1+\frac{u_1}{\gamma+d}\right)}\right) \\ \frac{\delta\left(1-\frac{\varepsilon d}{\alpha_1+d}\right)}{(\alpha+d)(d+\delta)}\left(1-\frac{d\left(1+\frac{u_1}{\gamma+d}\right)}{c\beta-\delta\left(1+\frac{u_1}{\gamma+d}\right)}\right) \end{pmatrix} Q \tag{17}$$

consistent with the uncontrolled case (5).

Moreover, as in the uncontrolled case, the solutions are admissible if they have non negative components. The first point, $\xi_1^e(u_1)$, clearly satisfies such condition for every $u_1 \geq 0$. For the second point, condition

$$c\beta - (d+\delta)\left(1+\frac{u_1}{\gamma+d}\right) \geq 0 \tag{18}$$

must be verified; it is the extension of (6) under u_1.

5.1.2. Stability analysis for $u_1 \neq 0$

The study of local stability for the equilibrium points (16) and (17) can be performed, as in the unforced case of Subsection 4.2, replacing f with $f + u_1 g_1$ (as in (3)). Then, the Jacobian matrix to be computed can be denoted by

$$J_{f+u_1 g_1}(\xi) = \frac{\partial(f+u_1 g_1)}{\partial \xi} \tag{19}$$

The evaluation of (19) in the equilibrium point $\xi_1^e(u_1)$ gives

$$A_1(u_1) = \left(\begin{array}{cc|ccc} -d-u_1 & \gamma & -c\beta\frac{1}{1+\frac{u_1}{\gamma+d}} & 0 & 0 \\ u_1 & -(\gamma+d) & 0 & 0 & 0 \\ \hline 0 & 0 & c\beta\frac{1}{1+\frac{u_1}{\gamma+d}} - (\delta+d) & 0 & 0 \\ 0 & 0 & \varepsilon\delta & -(\alpha_1+d) & 0 \\ 0 & 0 & (1-\varepsilon)\delta & \alpha_1 & -(\alpha+d) \end{array}\right) \tag{20}$$

The block structure helps once again to study the signs of the real parts of the eigenvalues. For the upper left block, the eigenvalues are obtained solving the characteristic equation

$$\lambda^2 + (\gamma + 2d + u_1)\lambda + d(\gamma + d + u_1) = 0 \tag{21}$$

The solutions $\lambda_1(u_1)$ and $\lambda_2(u_1)$ of equation (21) have always negative real part because the three coefficients are all positive for any admissible u_1. So

$$Re\,(\lambda_1(u_1)) < 0 \quad \text{and} \quad Re\,(\lambda_2(u_1)) < 0 \qquad \forall u_1 \in [0, +\infty)$$

For the bottom right triangular block, the eigenvalues are

$$\lambda_3(u_1) = c\beta\frac{1}{1+\frac{u_1}{\gamma+d}} - (\delta+d), \quad \lambda_4 = -(\alpha_1+d), \quad \lambda_5 - (\alpha+d) \tag{22}$$

While λ_4 and λ_5 are always real negative, the condition $c\beta\frac{1}{1+\frac{u_1}{\gamma+d}} - (\delta+d) < 0$ must be verified for $\lambda_3(u_1)$ as u_1 varies. It can be rewritten as

$$c\beta - (d+\delta)\left(1 + \frac{u_1}{\gamma+d}\right) < 0 \tag{23}$$

This condition and the one in (18) are mutually exclusive. Then, as in the unforced case, if $\xi_2^e(u_1)$ does not exist ((18) not verified), then $\xi_1^e(u_1)$ is locally asymptotically stable; otherwise, if $\xi_2^e(u_1)$ exist, $\xi_1^e(u_1)$ is an unstable equilibrium point. In this forced case, existence and stability of equilibrium points depend on u_1. Recalling the stability condition on the system parameters for the unforced dynamics in (9), it can be stated that if for the unforced system ξ_1^e is the only, stable, equilibrium point, the same holds for $\xi_1^e(u_1)$, $\forall u_1$; on the other hand, if $c\beta - (d+\delta) > 0$, that is ξ_2^e exists and ξ_1^e is unstable, it exists the value

$$u_{1,0} = (\gamma+d)\left(\frac{c\beta}{d+\delta} - 1\right) \tag{24}$$

such that

$$c\beta - (\delta+d)\left(1 + \frac{u_1}{\gamma+d}\right) < 0 \qquad \forall u_1 > u_{1,0} \tag{25}$$

Changing u_1, the transition from the conditions in which (23) holds, with one asymptotically stable equilibrium point $\xi_1^3(u_1)$, to the conditions with (23)

not true, with two equilibria $\xi_1^3(u_1)$ and $\xi_2^3(u_1)$, presents a bifurcation (Di Giamberardino et al. (2018)) at the point

$$\xi_{12}^e = \lim_{u_1 \to u_{1,0}} \xi_1(u_1) = \lim_{u_1 \to u_{1,0}} \xi_2(u_1) = \begin{pmatrix} \frac{d+\delta}{c\beta d} & \frac{c\beta-(d+\delta)}{c\beta d} & 0 & 0 & 0 \end{pmatrix}^T Q \quad (26)$$

In order to put in evidence such behaviours, a numerical case is introduced to depict the time histories of the state variables as u_1 changes.

The numerical values chosen for the model parameters are the same used in Di Giamberardino et al. (2018).

Parameter	Value		Parameter	Value
d	0.02		c	10
β	0.15		γ	0.2
δ	0.4		ψ	100000
ε	0.6		α_1	0.5
ϕ	0.95		α	1
Q	10^4			

Table 1: Numerical values of the model parameters

The initial conditions $\xi_0 = \begin{pmatrix} 92000 & 0 & 8000 & 0 & 0 \end{pmatrix}^T$ are used in all the numerical simulations, corresponding to the situation in which an infection is present but nobody knows it yet.

To help the interpretation of the results in the next Figures, the numerical values of the equilibrium points, for the set of parameters taken, are given:

$$\xi_1^e(u_1) = \begin{pmatrix} \frac{1}{0.02\left(1+\frac{u_1}{0.22}\right)} & \frac{\frac{u1}{0.22}}{0.02\left(1+\frac{u_1}{0.22}\right)} & 0 & 0 & 0 \end{pmatrix}^T Q \quad (27)$$

$$\xi_2^e(u_1) = \begin{pmatrix} \frac{1}{1.5-0.4\left(1+\frac{u_1}{0.22}\right)} \\ \frac{\frac{u_1}{0.22}}{1.5-0.4\left(1+\frac{u_1}{0.22}\right)} \\ 2.3810\left(1-\frac{0.02\left(1+\frac{u_1}{0.22}\right)}{1.5-0.4\left(1+\frac{u_1}{0.22}\right)}\right) \\ 1.0989\left(1-\frac{0.02\left(1+\frac{u_1}{0.22}\right)}{1.5-0.4\left(1+\frac{u_1}{0.22}\right)}\right) \\ 0.9122\left(1-\frac{0.02\left(1+\frac{u_1}{0.22}\right)}{1.5-0.4\left(1+\frac{u_1}{0.22}\right)}\right) \end{pmatrix} Q \quad (28)$$

with $c\beta - (d+\delta) = 1.08 > 0$, so that the uncontrolled dynamics has two equilibrium points, the first unstable and the second, the endemic condition, asymptotically stable. With $u_1 \neq 0$, the threshold value $u_{1,0}$ is $u_{1,0} = 0.5657$ and the bifurcation point ξ_{12}^e is

$$\xi_{12}^e = \begin{pmatrix} 1.4 \cdot 10^5 & 3.6 \cdot 10^5 & 0 & 0 & 0 \end{pmatrix}^T \quad (29)$$

Two sets of Figures show, separately, the different behaviours for values of u_1 smaller and greater than $u_{1,0}$: from Figure 1 to Figure 4 the case in which

$0 \leq u_1 \leq u_{1,0}$ is reported, while from Figure 5 to Figure 8 the case $u_1 \geq u_{1,0}$ is a referred.

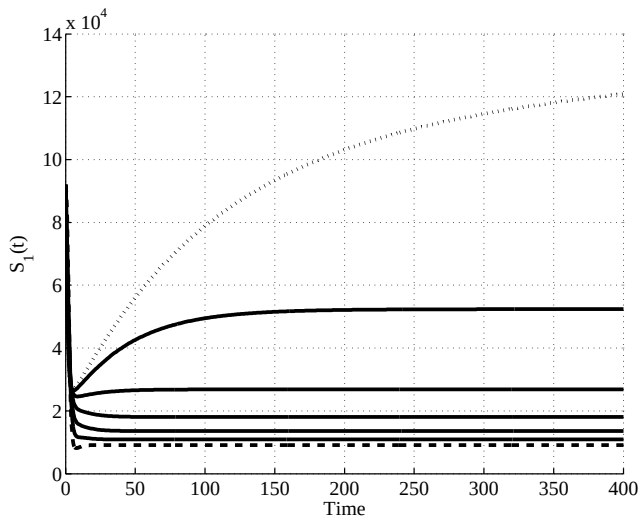

Figure 1: Time history of $S_1(t)$ for values $0 \leq u_1 \leq u_{1,0}$; the dashed corresponds to $u_1 = 0$, the dotted denotes the case $u_1 = u_{1,0}$

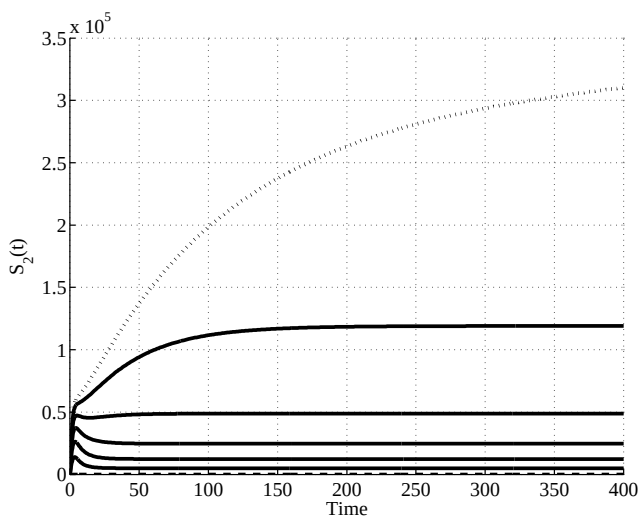

Figure 2: Time history of $S_2(t)$ for values $0 \leq u_1 \leq u_{1,0}$; the dashed corresponds to $u_1 = 0$, the dotted denotes the case $u_1 = u_{1,0}$

For the first set, the values $u_1 \in [0, 0.1, 0.20.30.4, 0.5, u_{1,0}]$ are considered. In each Figure from 1 to 4, the dashed line denotes the evolutions for $u_1 = 0$,

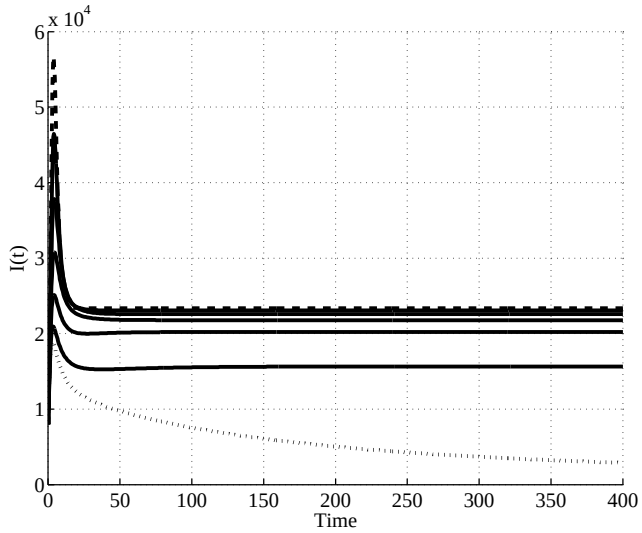

Figure 3: Time history of $I(t)$ for values $0 \leq u_1 \leq u_{1,0}$; the dashed corresponds to $u_1 = 0$, the dotted denotes the case $u_1 = u_{1,0}$

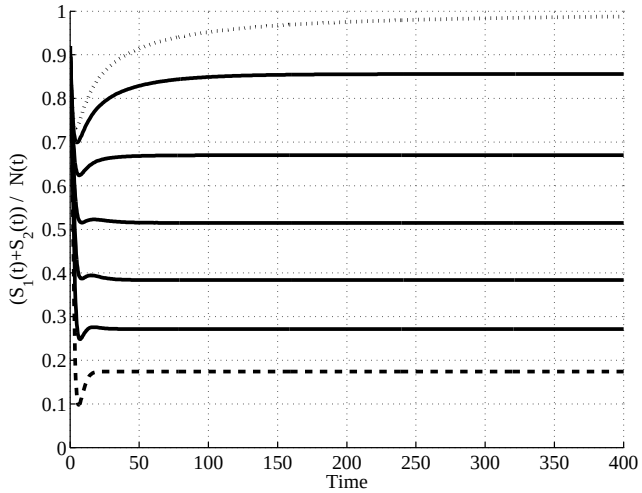

Figure 4: Time evolution of the relative number of healthy individuals $S_1(t) + S_2(t)$ w.r.t. the total population for values $0 \leq u_1 \leq u_{1,0}$; the dashed corresponds to $u_1 = 0$, the dotted denotes the case $u_1 = u_{1,0}$

while the dotted one represents the behaviours when $u_1 = u_{1,0}$. The five solid lines are associated to the intermediate values: they show a behaviour that uniformly goes from the uncontrolled one, dashed, to the bifurcation value for the control, dotted. Such a variation is increasing for $S_1(t)$ and $S_2(t)$, while it is

decreasing for $I(t)$. This means that, as u_1 increases, the parts of the population in $S_1(t)$ and $S_2(t)$, after an initial decrement, increases as well, showing, at each time, greater numbers for greater control amplitude and reaching, at steady state, greater numbers. Correspondingly, the infected population in $I(t)$ evolves following smaller values at each time, decreasing the steady state value as u_1 increases, till assuming zero as asymptotic value when u_1 is equal to the bifurcation value. The overall effect is the increment of the fraction of health population, depicted in Figure 4, reaching the full healthy condition as $u_1 \to u_{1,0}$.

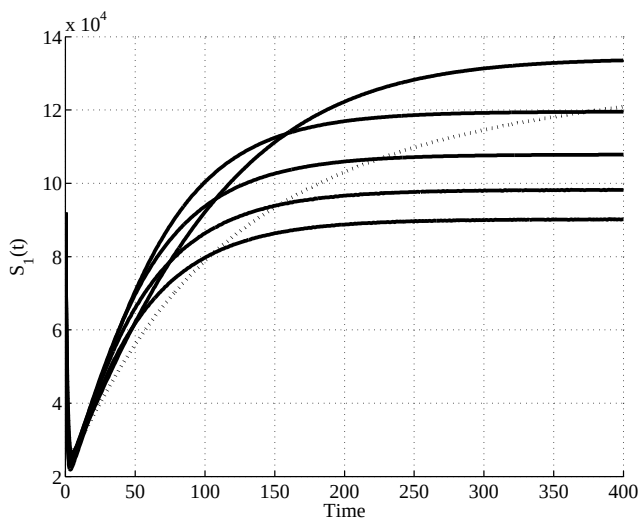

Figure 5: Time history of $S_1(t)$ for values $u_1 \geq u_{1,0}$

In the second set, the values $u_1 \in [u_{1,0}, 0.6, 0.7, 0.8, 0.9, 1]$ are considered. Also in this case, in each Figure from 5 to 8, the dotted line represents the behaviour when $u_1 = u_{1,0}$. As previously proved, for $u_1 > u_{1,0}$ the system has one equilibrium point only, the first one, and it is locally asymptotically stable. Then, according to the expression in (27), the behaviour of the state variable $S_1(t)$, for its steady state value, decreases as u_1 increases, and for the higher value simulated, $u_1 = 1$, it reaches the value $9.0164 \cdot 10^4$. At the same time, S_2 increases, as shown in Figure 6; for $u_1 = 1$, its steady state value is $4.0984 \cdot 10^5$, as expression (27) gives. The time history of $I(t)$, depicted in Figure 7, shows a faster convergence to zero as u_1 increases, always having zero as steady state value, according to (27). Then, all the population tends to be healthy, as Figure 8 shows.

For the study of local stability of $\xi_2^e(u_1)$ an analogous analysis must be performed, starting with the evaluation of (19) in such an equilibrium point.

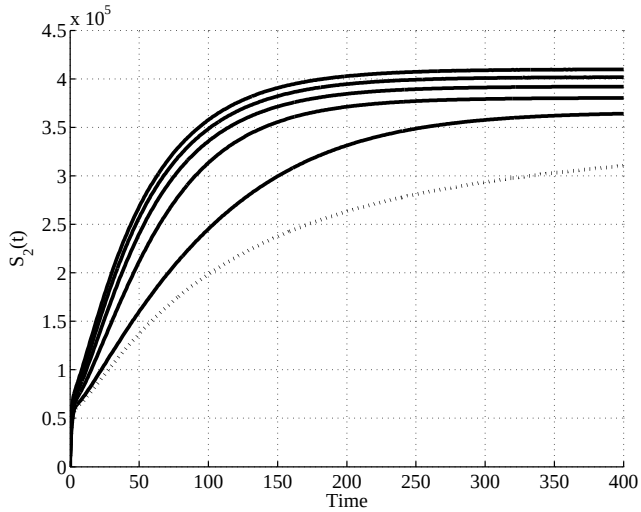

Figure 6: Time history of $S_2(t)$ for values $u_1 \geq u_{1,0}$

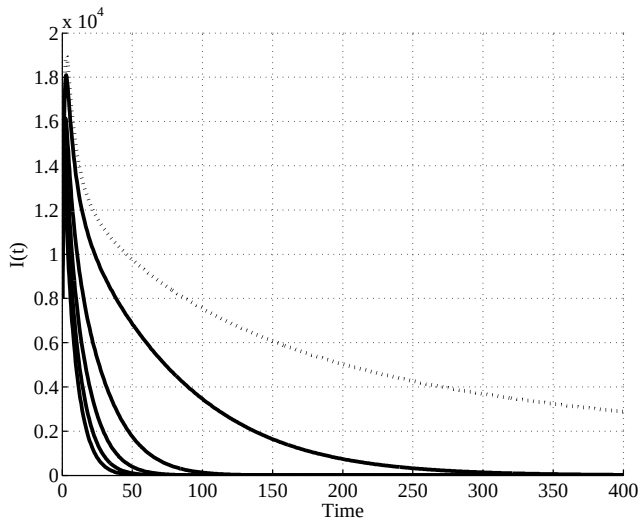

Figure 7: Time history of $I(t)$ for values $u_1 \geq u_{1,0}$

The result is the block triangular matrix

$$A_2(u_1) = \left(\begin{array}{c|c} A_2^{11} & 0 \\ \hline A_2^{21} & A_2^{22} \end{array} \right) \tag{30}$$

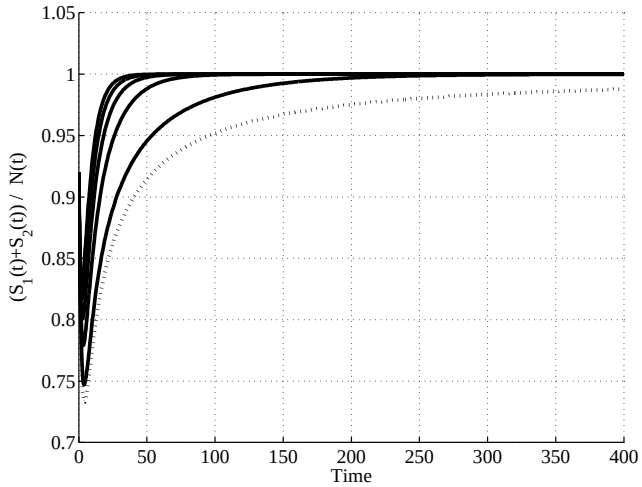

Figure 8: Time evolution of the relative number of healthy individuals $S_1(t)+S_2(t)$ w.r.t. the total population for values $u_1 \geq u_{1,0}$

with

$$A_2^{11}(u_1) = \begin{pmatrix} -(d+u_1)-c\beta\frac{I^e}{N_c^e}\left(1-\frac{S_1^e}{N_c^e}\right) & \gamma+c\beta\frac{S_1^e}{N_c^e}\frac{I^e}{N_c^e} & -c\beta\frac{S_1^e}{N_c^e}\left(1-\frac{I^e}{N_c^e}\right) \\ u_1 & -(\gamma+d) & 0 \\ c\beta\frac{I^e}{N_c^e}\left(1-\frac{S_1^e}{N_c^e}\right) & -c\beta\frac{S_1^e}{N_c^e}\frac{I^e}{N_c^e} & -(d+\delta)+c\beta\frac{S_1^e}{N_c^e}\left(1-\frac{I^e}{N_c^e}\right) \end{pmatrix} \tag{31}$$

$$A_2^{21} = \begin{pmatrix} 0 & 0 & \varepsilon\delta \\ 0 & 0 & (1-\varepsilon)\delta \end{pmatrix} \qquad A_2^{22} = \begin{pmatrix} -(\alpha_1+d) & 0 \\ \alpha_1 & -(\alpha+d) \end{pmatrix} \tag{32}$$

After some computations, the characteristic polynomial of matrix (31) can be written as

$$p(\lambda) = \lambda^3 + m_2\lambda^2 + m_1\lambda + m_0$$

with

$$\begin{aligned} m_2 &= \left(c\beta - \delta + (\gamma+d) + \frac{\gamma-\delta}{\gamma+d}u_1\right) \\ m_1 &= (c\beta-\delta)\left((\gamma+d) + \frac{(c\beta-(d+\delta))(d+\delta)}{c\beta}\right) + \\ &\quad +\delta u_1 - \frac{(d+\delta)^2(c\beta-\delta)}{c\beta(\gamma+d)}u_1 \\ m_0 &= -\frac{(d+\delta)(c\beta-(d+\delta))(\gamma+d)(c\beta-\delta)}{c\beta} + \\ &\quad +\frac{d+\delta}{c\beta}\left(dc\beta + 2\delta(c\beta-(d+\delta))\right)u_1 - \delta\frac{(d+\delta)^2}{c\beta(\gamma+d)}u_1^2 \end{aligned} \tag{33}$$

The conditions for the local stability of the equilibrium point (17) are

$$m_i > 0, \;\; i = 0,1,2 \text{ and } m_1 m_2 > m_0 \tag{34}$$

For the numerical case here referred, the equilibrium point is (28) and the Jacobian matrix (31) becomes

$$A_2^{11}(u_1) = \begin{pmatrix} -0.7976 + 0.3745u_1 & 0.5024 - 0.5345u_1 & -0.1176 - 0.5345u_1 \\ u_1 & -0.2200 & 0 \\ 0.7776 - 1.3745u_1 & -0.3024 + 0.5345u_1 & -0.3024 + 0.5345u_1 \end{pmatrix} \tag{35}$$

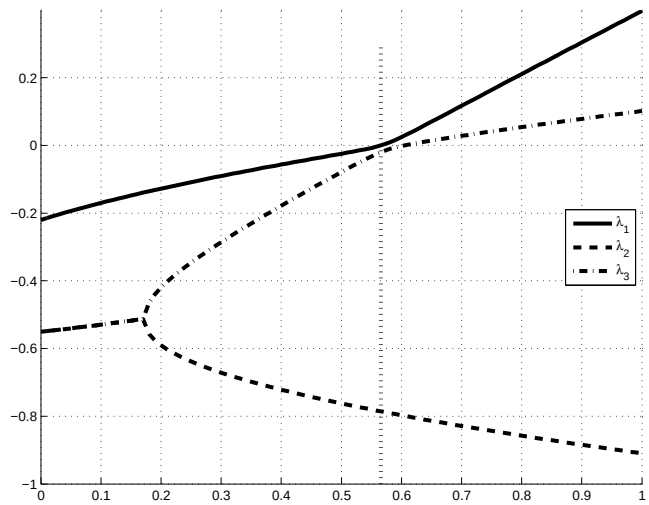

Figure 9: Real part of the eigenvalues of (35) for $u_1 \in [0, 1]$ are reported. The vertical dotted line denotes $u_{1,0} = 0.5657$, the bifurcation value

In Figure 9, the real part of the three eigenvalues of matrix (35) for values of $u_1 \in [0, 1]$ are reported. It can be seen that, for $u_1 < u_{1,0} = 0.5657$, highlighted in the Figure with the vertical dotted line, the linearised dynamics is asymptotically stable and then the equilibrium point $\xi_2^e(u_1)$ (17) exists as a second equilibrium point and it is asymptotically stable (the endemic condition). After that value, one eigenvalue becomes positive. The results of this analysis is that the equilibrium and the stability conditions of the dynamics (1) can be affected by external inputs, u_1 in this case, even making some stability properties lost.

In next Subsection, the same study is carried on for the input u_2, aiming at show whether the influence of the input on the stability is present for the second input too.

5.2. Analysis of the case $u_1(t) = u_3(t) = 0$ and $u_2(t) = u_2$

The case of a constant input $u_2 \neq 0$ is now considered in the present Subsection 5.2. As in Subsection 5.1, first the equilibrium points are computed and then their stability properties are studied.

5.2.1. Equilibria computation for $u_2 \neq 0$

In this case, to compute the new equilibria, the non linear system

$$f(S_1^e, S_2^e, I^e, P^e, A^e) + g_2(S_1^e, S_2^e, I^e, P^e, A^e)u_2 = 0 \tag{36}$$

has to be solved. It is the same as (4), with the addition of $g_2(\xi(t))u_2$, with g_2 as in (3). Performing the computations, the solution

$$\xi_1^e(u_2) = \begin{pmatrix} \frac{1}{d} & 0 & 0 & 0 & 0 \end{pmatrix}^T Q \tag{37}$$

is obtained; it does not depend on u_2 and it is the same as the unforced case ξ_1^e in (5). Moreover, once $S_2^e = 0$ is obtained, computations give also the expressions

$$I^e = \frac{c\beta - (d+\delta)}{d+\delta} S_1^e - \frac{\psi u_2}{d+\delta} \tag{38}$$

$$c\beta(\delta - c\beta)(S_1^e)^2 + (c\beta Q + \psi u_2(d + c\beta))\, S_1^e - \psi Q u_2 = 0 \tag{39}$$

Note that if $u_2 = 0$, from (38) one has the same condition on the uncontrolled case and, in fact, equation (39) reduces to a first order one, yielding the same solution as in (5). If $(\delta - c\beta) > 0$, the two roots of (39) are real, one positive and one negative; then, one value for the equilibrium point can be obtained, the positive root, say $S_1^{e_0}(u_2)$. On the other hand, if $(\delta - c\beta) < 0$, both the solutions have positive real part. They are real, and then they are equilibrium points, if and only if

$$(Qc\beta + \psi u_2(d + c\beta))^2 > 4c\beta Q\psi u_2 |\delta - c\beta| \tag{40}$$

If (40) is satisfied, two solutions $S_1^{e_1}(u_2)$ and $S_1^{e_2}(u_2)$ are obtained for equation (39). Then, for the first three components of the equilibrium points, three cases are possible, according to the values of the parameters and of the input u_2: i.) for $\delta - c\beta > 0$, one value for $S_1^e(u_2)$ is obtained, $S_1^{e_0}(u_2)$, solving (39) and taking the only positive solution; ii.) for $\delta - c\beta < 0$, if (40) holds, two solutions $S_1^{e_1}(u_2)$ and $S_1^{e_2}(u_2)$ are obtained solving (39); iii.) for $\delta - c\beta < 0$, if (40) doe not hold, no admissible (real) solutions are obtained from (39). Consequently, the corresponding values for the equilibrium $I^e(u_2)$ can be computed from (38) and denoted by $I^{e_i}(u_2)$, $i \in [0, 2]$ correspondingly to the value $S_1^{e-i}(u_2)$, while $S_2^e(u_2) = 0$ holds in any case. For the remaining two components $P^e(u_2)$ and $A^e(u_2)$, from (**??**) and (**??**), using (38), one has

$$P^{e_i}(u_2) = \left(\frac{\varepsilon\delta}{\alpha_1 + d} + \frac{\phi\psi}{(\alpha_1 + d)\,(S_1^{e_i}(u_2) + I^{e_i})} u_2 \right) I^{e_i} \tag{41}$$

$$A^{e_i}(u_2) = (1-\varepsilon)\delta I^{e_i}(u_2) + \alpha_1 P^{e_i}(u_2) + \frac{(1-\phi)\psi I^{e_i}(u_2)}{(\alpha + d)\,(S_1^{e_i}(u_2) + I^{e_i}(u_2))} u_2 \tag{42}$$

The equilibrium points $\xi_2^{e_i}(u_2)$ can then be written as

$$\xi_2^{e_i}(u_2) = \begin{pmatrix} S_1^{e_i}(u_2) & 0 & I^{e_i}(u_2) & P^{e_i}(u_2) & A^{e_i}(u_2) Q \end{pmatrix}^T \tag{43}$$

5.2.2. Stability analysis for the equilibrium $\xi_1^e(u_2)$

Once again, the study of local stability for the equilibrium points (37) and (43) can be performed referring to their linear approximations. The study for $\xi_1^e(u_2)$ in (37) gives the matrix

$$A_1(u_2) = \left(\begin{array}{ccc|cc} -d & \gamma & -c\beta & 0 & 0 \\ 0 & -(\gamma+d) & 0 & 0 & 0 \\ 0 & 0 & c\beta-(\delta+d)-\psi u_2 & 0 & 0 \\ \hline 0 & 0 & \varepsilon\delta+\phi\psi u_2 & -(\alpha_1+d) & 0 \\ 0 & 0 & (1-\varepsilon)\delta+(1-\phi)\psi u_2 & \alpha_1 & -(\alpha+d) \end{array}\right) \tag{44}$$

Then, in addition to the four constant negative eigenvalues $\lambda_1 = -d$, $\lambda_2 = -(\gamma+d)$, $\lambda_3 = -(\alpha_1+d)$ and $\lambda_4 = -(\alpha+d)$, there is one eigenvalue which is function of the input u_2, $\lambda_5 = c\beta-(d+\delta)-\psi u_2$. If $c\beta-(d+\delta) < 0$, the same as (9), then $\lambda_5 < 0\ \forall u_2 \geq 0$. On the other hand, if condition (9) is not verified for the uncontrolled system, there exists a value $u_{2,0} = \frac{c\beta-(d+\delta)}{\psi}$ such that $\lambda_5 < 0\ \forall u_2 > u_{2,0}$. This means that a system for which the parameters are such that the equilibrium ξ_1^e is unstable, under the action of an input u_2 it can become stable. Once more, the effect of a control input, in this case u_2 can affect the stability properties of a system (1).

5.2.3. Stability analysis for the equilibrium $\xi_2^{e_i}(u_2)$

On the basis of the discussion in Subsection 5.2.1, the existence, and hence the stability, of the equilibrium points $\xi_2^{e_i}(u_2)$ (43), are highly dependent on the values of the system parameters. Then, an analytical study of their stability involves long and complicated expressions, not useful for qualitative discussions. To show the effects of an input u_2 on the existence and the stability of the points (43), a numerical analysis is here performed, making use of the already introduced values in Table 1.

Numerical simulations are performed for $u_1 = u_3 = 0$ and for values of u_2 in the set $u_2 \in \{0, 0.2, 0.4, 0.6, 0.8, 1\}$. Some of the result are reported in Figures 10–17. In alL of them, the case $u_2 = 0$, the uncontrolled case, is depicted by the dashed line, for comparative purpose with the other increasing values. Figures 10 and 11 show the time histories of the two state components $S_1(t)$ and $I(t)$, for the different input values. While the result of monotonically increment of the individuals $S_1(t)$ as u_2 increases is expected, as well as the corresponding decrement for the infected subjects $I(t)$, there are two interesting results which the Figures show. The first is the oscillatory behaviour that appears and that is related to the amplitude of the input u_2. This kind of time evolution is well evidenced once referring to Figure 14, where the trajectories in the plane $I(t) + P(t) + A(t)$ vs. $S_1(t) + S_2(t)$ is plotted: the spiral trajectory while converging to the equilibrium point is clearly visible. This means that, under input $u_2 \neq 0$, there are time instants in which the number of the infected individuals $I(t)$ can seem greater than expected, but it is related to the transient behaviour only. The second results put in evidence from the numerical results is

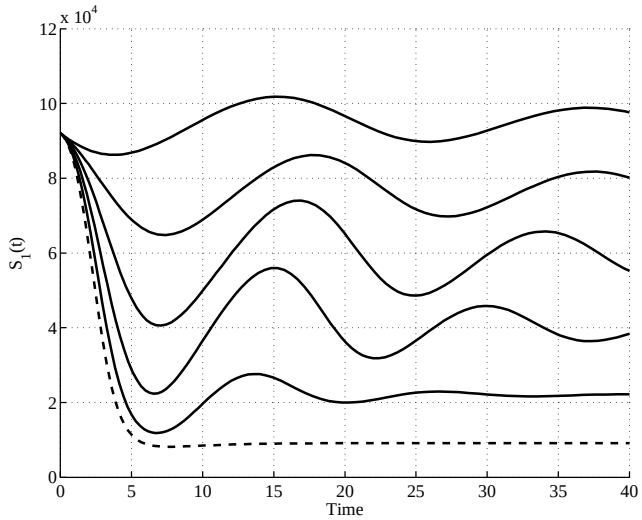

Figure 10: Time history of $S_1(t)$ for $u_2 \in \{0, 0.2, 0.4, 0.6, 0.8, 1\}$. The dashed line depicts the case $u_2 = 0$, the behaviours change monotonically with u_2.

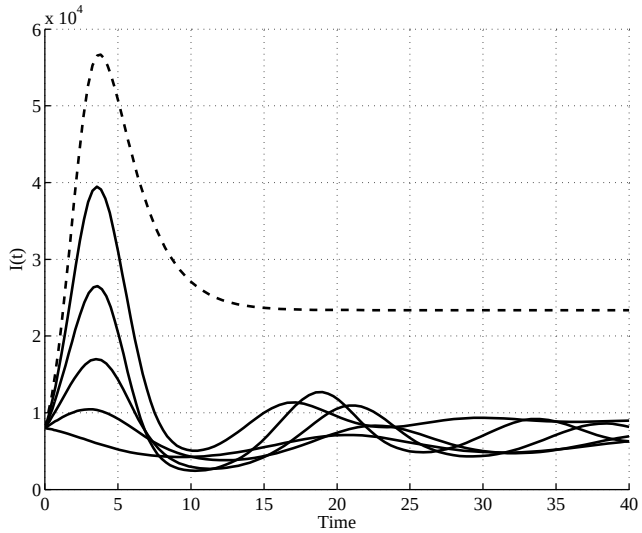

Figure 11: Time history of $I(t)$ for $u_2 \in \{0, 0.2, 0.4, 0.6, 0.8, 1\}$. The dashed line depicts the case $u_2 = 0$, the behaviours change monotonically with u_2.

that the number of diagnosed infected individuals $P(t)$ and $A(t)$ do not decrease as $I(t)$ decreases. This is due to the fact that the action of the control u_2 aims at increasing the number of diagnoses, so that while $I(t)$ decreases, people moves to $P(t)$ (Figure 12) and $A(t)$ (Figure 13). The overall effects on the

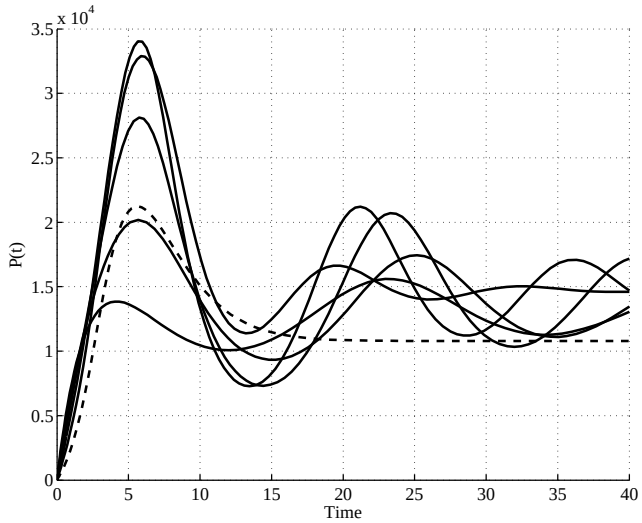

Figure 12: Time history of $P(t)$ for $u_2 \in \{0, 0.2, 0.4, 0.6, 0.8, 1\}$. The dashed line depicts the case $u_2 = 0$, the behaviours change monotonically with u_2.

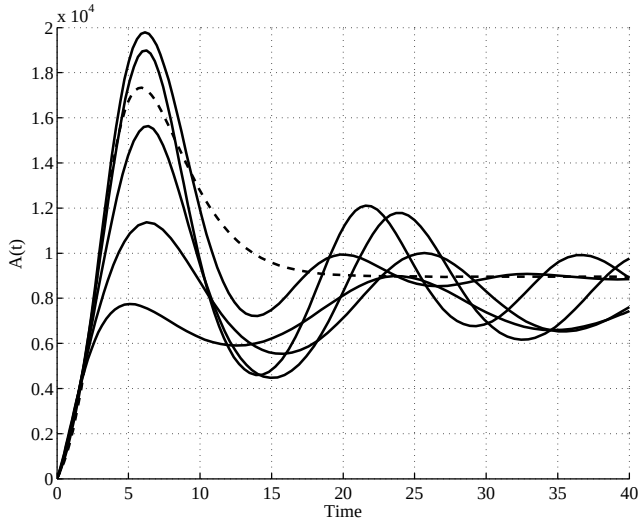

Figure 13: Time history of $A(t)$ for $u_2 \in \{0, 0.2, 0.4, 0.6, 0.8, 1\}$. The dashed line depicts the case $u_2 = 0$, the behaviours change monotonically with u_2.

total population can be seen in Figure 15, where its increment is clear. While the total population increases, the fraction of healthy people $S_1(t) + S_2(t)$ with respect to the total population strongly increases, as reported in Figure 16 and, at the same time, the fraction of diagnosed patients $P(t) + A(t)$ significantly decreases, Figure 17.

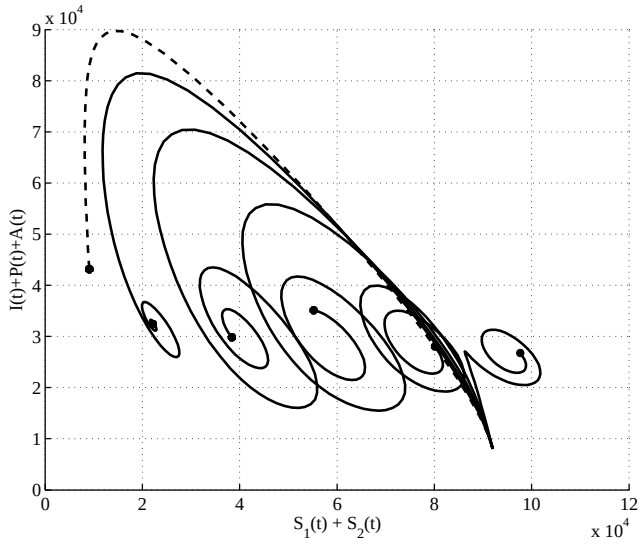

Figure 14: Time history of $A(t)$ for $u_2 \in \{0, 0.2, 0.4, 0.6, 0.8, 1\}$. The dashed line depicts the case $u_2 = 0$, the behaviours change monotonically with u_2.

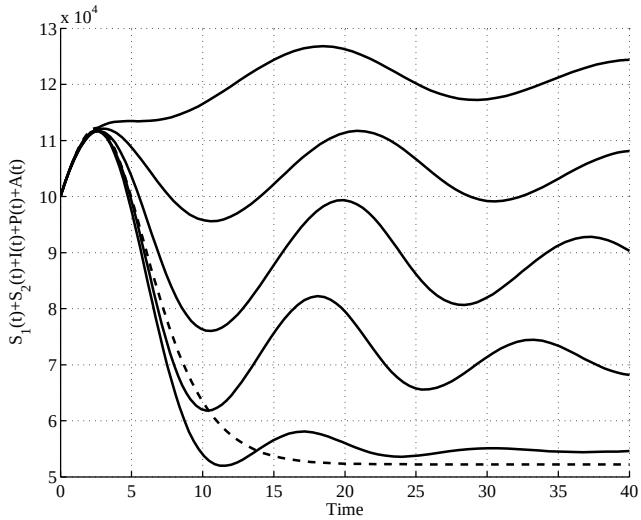

Figure 15: Time evolution of the total population, for $u_2 \in \{0, 0.2, 0.4, 0.6, 0.8, 1\}$. The dashed line depicts the case $u_2 = 0$, the behaviours change monotonically with u_2.

6. The interactions between populations

The study of the effects on a population of the interactions with different groups can be performed modelling the whole population as the aggregate of each one and introducing terms in the dynamics which take into account the

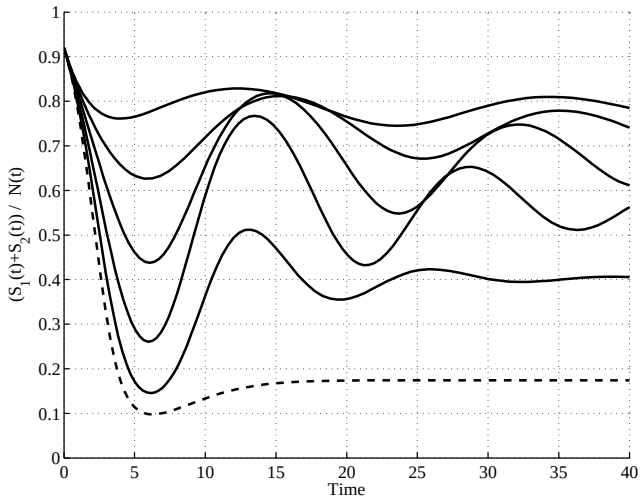

Figure 16: Time evolution of the healthy individuals $S_1(t) + S_2(t)$ with respect to the total population, for $u_2 \in \{0, 0.2, 0.4, 0.6, 0.8, 1\}$. The dashed line depicts the case $u_2 = 0$, the behaviours change monotonically with u_2.

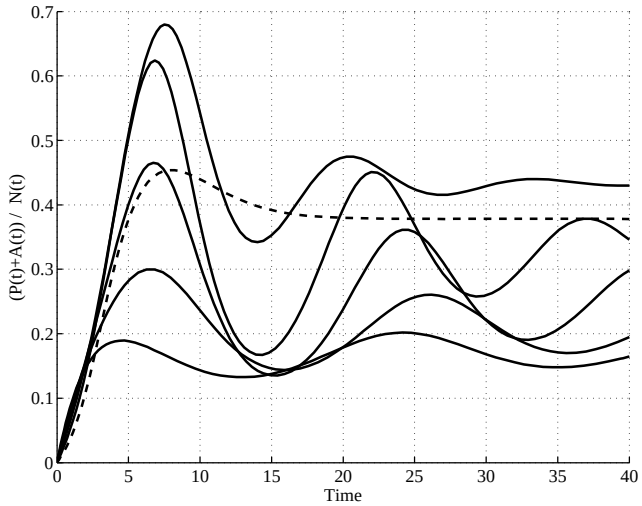

Figure 17: Time evolution of the diagnosed patients $P(t) + A(t)$ with respect to the total population, for $u_2 \in \{0, 0.2, 0.4, 0.6, 0.8, 1\}$. The dashed line depicts the case $u_2 = 0$, the behaviours change monotonically with u_2.

possible interconnections. For the dynamics (1) considered in Section 3, this would bring to a $5N$ dimensional system, being N the number of groups considered. A characterisation of the entire population could be then possible highly increasing the complexity of the whole expression.

Taking one of the N population and considering all the interactions with the remaining $N-1$ ones by means of global averaged terms, the mathematical model can be strongly simplified introducing changes in (1) which can take into account the combined effects of the external interactions. Clearly, many details are lost since some contributions are averaged, but a useful preliminary analysis can be performed. On the basis of the results obtained for the single group model in previous Sections, the evidence and the effects of the changes introduced in a population by the interactions with external world can be obtained once such interactions are suitably modelled as additional inputs and/or changes in the parameter values. Concerning the additional inputs, these can be assumed as the sum of the effects of migration, positive and negative, between the group under investigation with respect to all the other ones. Such effects can be modelled as constant fluxes, which introduce additive constant terms in the dynamics, or can be supposed driven by some characteristic of the group behaviour, such as a *higher* or *lower* level of healthy, for example.

Migrations can affect also the value of some parameters, representing changes in the behaviour od some individuals consequent to some cultural modifications. Examples are c and β, for the number of the contagious interactions, depending also on cultural and educational facts, γ for the attitude of ignoring the dangerous effects of some kind of relationships, and so on.

In the present study, the assumption that the healthy status of a population can be an indicator of its attractiveness, being related to the richness, the higher social level and so on, the changes introduced in the model (1) to take into account the interactions with other groups are represented by the introduction of additional terms of the form $f_i(S_1, S_2, I, P, A)$, $i = 1$ for S_1, $i = 2$ for S_2 and $i = 3$ for I, assuming that known infected individuals P and A are not allowed to migrate. Then, (1) becomes

$$\dot{S}_1(t) = Q - dS_1(t) - \frac{c\beta S_1(t)I(t)}{N_c(t)} + \gamma S_2(t) - S_1(t)u_1(t) + f_1(S_1, S_2, I, P, A) \tag{45a}$$

$$\dot{S}_2(t) = -(\gamma + d)S_2(t) + S_1(t)u_1(t) + f_2(S_1, S_2, I, P, A) \tag{45b}$$

$$\dot{I}(t) = \frac{c\beta S_1(t)I(t)}{N_c(t)} - (d + \delta)I(t) - \psi\frac{I(t)}{N_c(t)}u_2(t) + f_3(S_1, S_2, I, P, A) \tag{45c}$$

$$\dot{P}(t) = \varepsilon\delta I(t) - (\alpha_1 + d)P(t) + \phi\psi\frac{I(t)}{N_c(t)}u_2(t) + P(t)u_3(t) \tag{45d}$$

$$\dot{A}(t) = (1-\varepsilon)\delta I(t) + \alpha_1 P(t) - (\alpha + d)A(t) + (1-\phi)\psi\frac{I(t)}{N_c(t)}u_2(t) - P(t)u_3(t) \tag{45e}$$

Some choices for the $f_i(S_1, S_2, I, P, A)$, under the assumption previously mentioned, can be, for example, proportional to $\frac{S_1+S_2+I}{S_1+S_2+I+P+A}$, meaning that the more the group is healthy, the more it is attractive, or proportional to $-\frac{P+A}{S_1+S_2+I+P+A}$, meaning that the higher is the number of the infectious patients, the more it is repulsive. Simplified versions can be considered neglecting

the normalising denominators. In next section, the choice

$$f_i(S_1, S_2, I, P, A) = m_i \frac{S_1 + S_2 + I}{N} - n_i \frac{P + A}{N} \tag{46}$$

is adopted, $i = 1, 2, 3$, where $N = S_1 + S_2 + I + P + A$.

This corresponds to introduce, in the most general formulation, both an immigration term

$$m_i \frac{S_1 + S_2 + I}{S_1 + S_2 + I + P + A} \tag{47}$$

and an emigration one

$$n_i \frac{P + A}{S_1 + S_2 + I + P + A} \tag{48}$$

to each of the involved dynamics, the ones for S_1, S_2 and I. In this case, the effects of the migration fluxes vary according to the values of the six parameters m_i and n_i.

6.1. Equilibria under external interactions

In this Subsection, the effects on the equilibrium conditions of the external interactions just introduced are studied. A full analysis should be performed studying the effect of the changes of the new six parameters on the dynamics behaviour. In order to better identify the relationships between each contribution and the corresponding effect, the analysis is performed isolating some particular fluxes. In particular, two cases are separately addressed. The first supposes that the contribution of the immigration/emigration flux acts on the susceptible group S_1 only, aiming at analysing what may happen when the number of uninfected people changes due to migrations. The second one is, in some sense, the dual case: the effects of the migration are evaluated under the hypothesis that all the flux is concentrated on the infected but not diagnosed individuals I. With respect to the model here introduced for the interactions (45), in the terms (46), $m_2 = m_3 = n_2 = n_3 = 0$ are chosen for the first case investigated, while $m_1 = m_3 = n_1 = n_3 = 0$ are assumed for the second case.

Equilibrium points and their stability are firstly analysed, in order to characterise the dynamical properties and to be able to compare the results with the isolated group case of Section 3.

6.1.1. Equilibrium points and stability properties for the case of health population migration

Under the hypothesis previously described, in this case the equilibrium points are computed solving the non linear system

$$
\begin{aligned}
Q - dS_1^e - \frac{c\beta S_1^e I^e}{N_c^e} + \gamma S_2^e + m_1 \frac{S_1^e + S_2^e + I^e}{N^e} - n_1 \frac{P^e + A^e}{N^e} &= 0 \quad (49)\\
-(\gamma + d) S_2^e &= 0 \quad (50)\\
\frac{c\beta S_1^e I^e}{N_c^e} - (d+\delta) I^e &= 0 \quad (51)\\
\varepsilon\delta I^e - (\alpha_1 + d) P^e &= 0 \quad (52)\\
(1-\varepsilon)\delta I^e + \alpha_1 P^e - (\alpha + d) A^e &= 0 \quad (53)
\end{aligned}
$$

One solution is given by

$$
\xi_1^e(m_1, n_1) = \begin{pmatrix} \frac{Q+m_1}{d} & 0 & 0 & 0 & 0 \end{pmatrix}^T \tag{54}
$$

Then, setting

$$
P^e + A^e = \frac{\delta}{\alpha_1 + d} \left(\frac{\varepsilon\alpha + \alpha_1 + d}{\alpha + d} \right) I^e = \pi I^e \tag{55}
$$

and performing some computations, the second solution

$$
\xi_2^e(m_1, n_1) = \begin{pmatrix} \frac{Q}{c\beta-\delta} + \frac{m_1 c\beta - n_1 \pi (c\beta - (d+\delta))}{(c\beta(1+\pi) - \pi(d+\delta))(c\beta-\delta)} \\ 0 \\ \frac{c\beta-(d+\delta)}{d+\delta} \left(\frac{Q}{c\beta-\delta} + \frac{m_1 c\beta - n_1 \pi (c\beta - (d+\delta))}{(c\beta(1+\pi) - \pi(d+\delta))(c\beta-\delta)} \right) \\ \frac{\varepsilon\delta}{\alpha_1+d} \frac{c\beta-(d+\delta)}{d+\delta} \left(\frac{Q}{c\beta-\delta} + \frac{m_1 c\beta - n_1 \pi (c\beta - (d+\delta))}{(c\beta(1+\pi) - \pi(d+\delta))(c\beta-\delta)} \right) \\ \frac{\delta(\alpha_1 + d(1-\varepsilon))}{(\alpha+d)(\alpha_1+d)} \frac{c\beta-(d+\delta)}{d+\delta} \left(\frac{Q}{c\beta-\delta} + \frac{m_1 c\beta - n_1 \pi (c\beta - (d+\delta))}{(c\beta(1+\pi) - \pi(d+\delta))(c\beta-\delta)} \right) \end{pmatrix} \tag{56}
$$

is obtained. The existence of this solution depends on the coefficients m_1 and n_1, since it must be verified that $S_1^e \geq 0$. However, once the condition on S_1^e is satisfied, from $I^e \geq 0$ the condition $c\beta - (d+\delta) \geq 0$ must holds. This is the same as (6) for ξ_2^e in Subsection 4.1. Expression (56) can be simplified writing

$$
\xi_2^e(m_1, n_1) = \begin{pmatrix} C_0 + C_m m_1 - C_n n_1 \\ 0 \\ K_I \left(C_0 + C_m m_1 - C_n n_1 \right) \\ K_P \left(C_0 + C_m m_1 - C_n n_1 \right) \\ K_A \left(C_0 + C_m m_1 - C_n n_1 \right) \end{pmatrix} \tag{57}
$$

once the following coefficients are defined

$$C_0 = \frac{Q}{c\beta - \delta} \tag{58}$$

$$C_m = \frac{c\beta}{(c\beta(1+\pi) - \pi(d+\delta))(c\beta - \delta)} \tag{59}$$

$$C_n = \frac{\pi(c\beta - (d+\delta))}{(c\beta(1+\pi) - \pi(d+\delta))(c\beta - \delta)} \tag{60}$$

$$K_I = \frac{c\beta - (d+\delta)}{d+\delta} \tag{61}$$

$$K_P = \frac{\varepsilon\delta}{\alpha_1 + d} K_I \tag{62}$$

$$K_A = \frac{\delta\,(\alpha_1 + d(1-\varepsilon))}{(\alpha+d)(\alpha_1+d)} K_I \tag{63}$$

The structure of expression (57) shows that the equilibrium point linearly change w.r.t. both m_1 and n_1.

The study of the stability characteristics for the two equilibrium points is performed, once again, analysing the stability of the linearised dynamics in the neighbourhood of the equilibria. For the first point $\xi_1^e(m_1, n_1)$, the Jacobian matrix computed in the equilibrium point is the same as for the isolated unforced case ξ_1^e in (5). Its expression is given in (7) and the same stability conditions can be obtained: the equilibrium point $\xi_1^e(m_1, n_1)$ is locally asymptotically stable under the condition (9). For the second equilibrium point $\xi_2^e(m_1, n_1)$ in (57), the dynamical matrix of the linear approximation has the structure

$$A_2(m_1, n_1) = \left(\begin{array}{c|c} A_2^{11}(m_1, n_1) & 0 \\ \hline A_2^{21}(m_1, n_1) & A_2^{22}(m_1, n_1) \end{array} \right) \tag{64}$$

with $A_2^{22}(m_1, n_1)$ equal to the one in (12) for the isolated unforced case, for which the two eigenvalues, $\lambda_4 = -(\alpha_1 + d)$ and $\lambda_5 = -(\alpha + d)$ are real negative. Then, for the stability conditions, matrix

$$A_2^{11}(m_1, n_1) = \begin{pmatrix} -d - c\beta\frac{K_I^2}{(1+K_I)^2} & \gamma + c\beta\frac{K_I}{(1+K_I)^2} & -c\beta\frac{1}{(1+K_I)^2} \\ 0 & -(\gamma+d) & 0 \\ c\beta\frac{K_I^2}{(1+K_I)^2} & -c\beta\frac{K_I}{(1+K_I)^2} & c\beta\frac{1}{(1+K_I)^2} - (d+\delta) \end{pmatrix} \tag{65}$$

must be analysed. It is interesting to note that it does not depend on the coefficients m_1 or n_1; then, the same holds for the stability of the equilibrium points obtained varying such coefficients. One of the eigenvalues of (65), $\lambda_3 = -(\gamma + d) < 0$, is evident from the structure. The other two can be computed as the roots of the polynomial equation

$$\lambda^2 + \left(d + (d+\delta) - c\beta\frac{1 - K_I^2}{(1+K_I)^2} \right)\lambda + \left(d(d+\delta) + c\beta\frac{(d+\delta)K_I^2 - d}{(1+K_I)^2} \right) \tag{66}$$

or, replacing the full expression for K_I and performing all the simplifications,

$$\lambda^2 \quad + \quad (c\beta-\delta)\lambda+(d+\delta)(c\beta-\delta)\frac{c\beta-(d+\delta)}{c\beta}=0 \tag{67}$$

which is the same as (13). On the basis of the discussion in Subsection 4.2, it is possible to conclude that the condition for the local asymptotic stability for $\xi_2^e(m_1,n_1)$ does not depend on m_1 and n_1 and it is the same given in (14). Moreover, the same relationships between existence and stability of the two equilibrium points, as the ones in Subsection 4.2 for ξ_1^e and ξ_2^e, hold.

6.1.2. Equilibrium points and stability properties for the case of infected population migration

Following the same procedure as in the previous cases, the equilibrium points are computed solving the non linear system

$$\begin{aligned}
Q-dS_1^e-\frac{c\beta S_1^e I^e}{N_c^e}+\gamma S_2^e &= 0 && (68)\\
-(\gamma+d)S_2^e &= 0 && (69)\\
\frac{c\beta S_1^e I^e}{N_c^e}-(d+\delta)I^e+m_3\frac{S_1^e+S_2^e+I^e}{N^e}-n_3\frac{P^e+A^e}{N^e} &= 0 && (70)\\
\varepsilon\delta I^e-(\alpha_1+d)P^e &= 0 && (71)\\
(1-\varepsilon)\delta I^e+\alpha_1 P^e-(\alpha+d)A^e &= 0 && (72)
\end{aligned}$$

From equation (69) $S_2^e=0$ is immediately obtained. Once that $N_c^e=S_1^e+I^e$ and $N^e=S_1^e+(1+\pi)I^e=N_c^e+\pi I^e$ are introduced, the system to be solved can be reduced to the equations (68) and (70), rewritten as

$$\begin{aligned}
Q-dS_1^e-\frac{c\beta S_1^e I^e}{S_1^e+I^e} &= 0 && (73)\\
\frac{c\beta S_1^e I^e}{S_1^e+I^e}-(d+\delta)I^e+m_3\frac{S_1^e+I^e}{S_1^e+(1+\pi)I^e}-n_3\frac{\pi I^e}{S_1^e+(1+\pi)I^e} &= 0 && (74)
\end{aligned}$$

From (73), one can write

$$I^e=\frac{(dS_1^e-Q)}{Q-(c\beta+d)S_1^e}S_1^e \tag{75}$$

while, for S_1^e, after computations one gets the polynomial equation

$$a_3\left(S_1^e\right)^3+a_2\left(S_1^e\right)^2+a_1S_1^e+a_0=0 \tag{76}$$

whose coefficients are

$$\begin{aligned}
a_3 &= d(c\beta-\delta)(c\beta-\pi d)\\
a_2 &= 2\pi Qd(c\beta-\delta)-(c\beta+d)(c\beta(Q+m_3)+\pi dn_3)+Qc\beta\delta+\pi Qd^2\\
a_1 &= c\beta Q\left(Q(1-\pi)+m_3+\pi n_3\right)+\pi Q^2\delta)-2\pi Qd\left(Q-n_3\right) && (77)\\
a_0 &= \pi Q^2\left(Q-n_3\right)
\end{aligned}$$

The feasible solutions correspond to the real positive roots of polynomial (76). Conditions should be given for the coefficients to characterise the roots in order to have admissible solutions but they are not easy to be written and their analysis requires a numerical evaluation of such conditions. Then, from now on, the numerical values reported in Table 1 are used, to show a possible behaviour and also for comparative purpose with all the results and the discussions given in the previous Section 5.

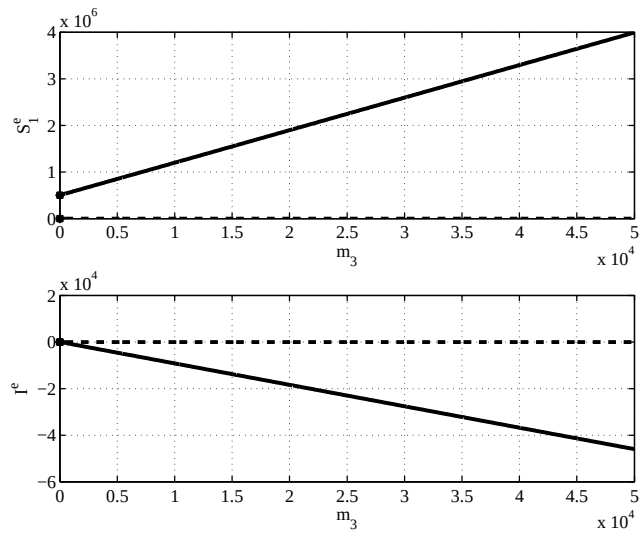

Figure 18: Values of the first solution S_1^e of (76) and I^e in (75) for $m_3 \in [0, 5\,10^4]$

With the parameters given in Table 1, the coefficients (77) assume the following expression depending on the two parameters m_3 and n_3,

$$a_3 = 0.0326 \tag{78}$$

$$a_2 = -2.2800m_3 - 0.0257n_3 - 1.6425 \cdot 10^4 \tag{79}$$

$$a_1 = 15000m_3 + 1.3008 \cdot 10^4 n_3 + 5.3710 \cdot 10^7 \tag{80}$$

$$a_0 = -8.4465 \cdot 10^7 n_3 + 8.4465 \cdot 10^{11} \tag{81}$$

The three solutions of equation (76) are computed for different values of $m_3 \in [0,\ 5 \cdot 10^4]$ and $n_3 \in [0,\ 5 \cdot 10^4]$. In Figures 18, 19 and 20 the variations of such solutions with respect to of m_3 are reported, keeping $n_3 = 0$, while Figures 21, 22 and 23 depict how the solutions vary according to different values of n_3 with $m_3 = 0$. In each Figure, the solid line represents the real part of the solution and the dashed line denotes the imaginary part, so that it is easy to reject the solutions which are not consistent with the real condition of the state variables. In all the six Figures, it can be checked that the values of the equilibrium components S_1^e and I^e are all real. Moreover, in order to be admissible values, the components of the state must be non negative. In this

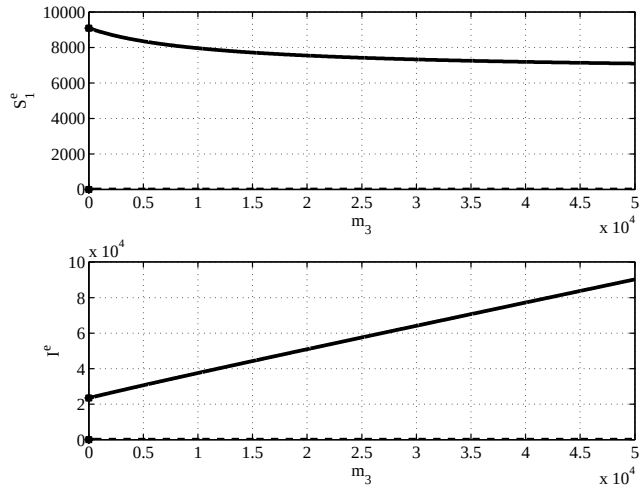

Figure 19: Values of the second solution S_1^e of (76) and I^e in (75) for $m_3 \in [0, 5\,10^4]$

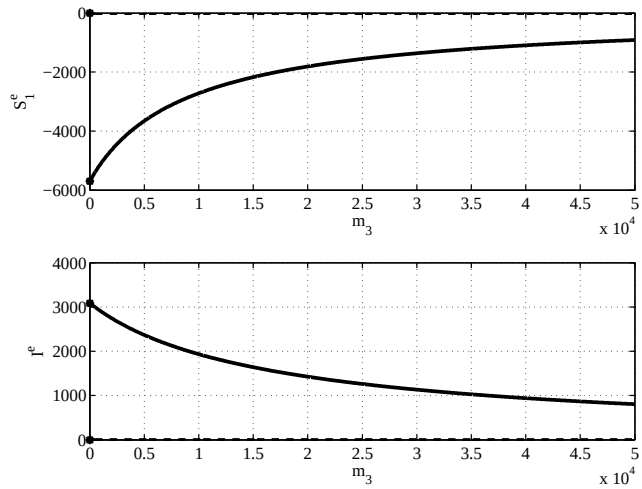

Figure 20: Values of the third solution S_1^e of (76) and I^e in (75) for $m_3 \in [0, 5\,10^4]$

case, for the range of values for the parameters m_3 and n_3 considered, it can be seen that keeping $n_3 = 0$, the three roots S_1^e of the polynomial (76) are real, two positive, Figures 18 and 19, and one negative, Figure 20 for all the values given to $m_3 \in [0, 5\,10^4]$. The corresponding values for the equilibrium I^e are negative for the first solution in Figure 18 and positive for the remaining two cases, Figures 19 and 20. Then, while for $m_3 = n_3 = 0$ the first and the second solutions are admissible, as m_3 increases, only the second is a feasible solution; in this case, only one equilibrium point exists and its components S_1^e and I^e are

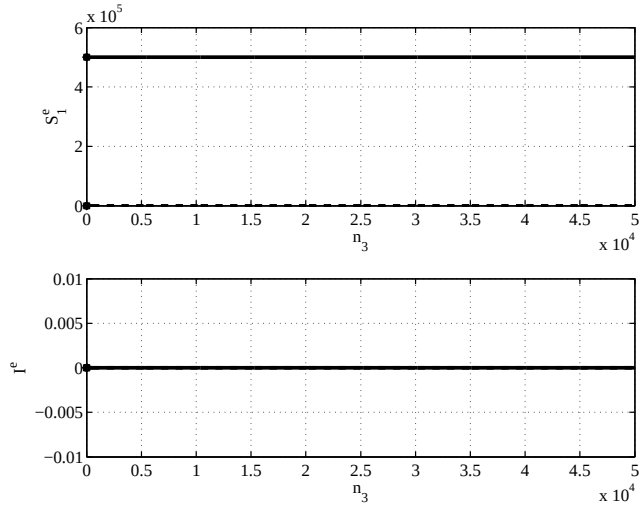

Figure 21: Values of the first solution S_1^e of (76) and I^e in (75) for $n_3 \in [0, 5\,10^4]$

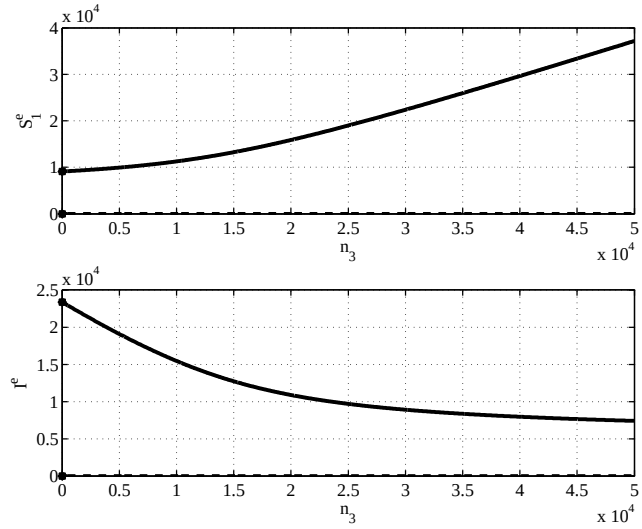

Figure 22: Values of the second solution S_1^e of (76) and I^e in (75) for $n_3 \in [0, 5\,10^4]$

given in Figure 19 for each value of m_3 in the range considered.

On the other hand, varying n_3 while $m_3 = 0$, the first solution, depicted in Figure 21, shows that n_3 does not influence one of the equilibrium point of the non interacting case, defined in Section 4.1 as ξ_1^e. Also the second solution, plotted in Figure 22, is admissible, since both S_1^e and I^e are positive for all the values considered for n_3. On the contrary, the third solution cannot be assumed

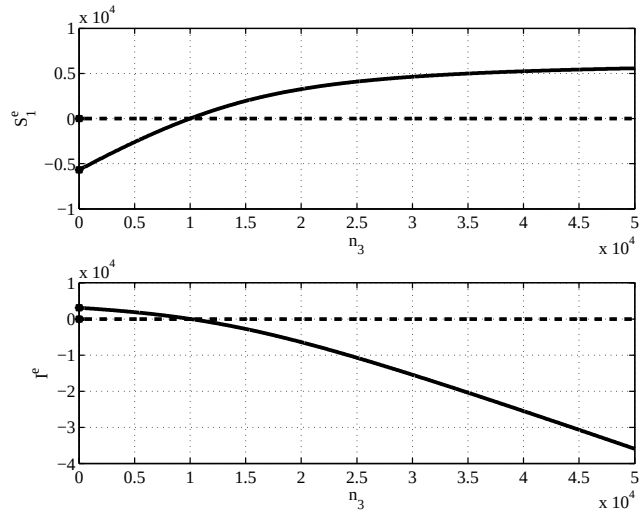

Figure 23: Values of the third solution S_1^e of (76) and I^e in (75) for $n_3 \in [0, 5\,10^4]$

as an equilibrium point, since when S_1^e is positive, I^e is negative. Moreover, the value $S_1^e = 0$ is never acceptable since it does not satisfy equation (73).

A stability analysis for the equilibrium points just computed is performed necessarily on the numerical case addressed till now. The Jacobian matrix $J_f(\xi) = \frac{\partial f}{\partial \xi}$ must be computed and then evaluated et each equilibrium point. Since the structure of the system is the same as (1) with the additional term

$$m_3 \frac{S_1 + S_2 + I}{N} - n_3 \frac{P + A}{N} \tag{82}$$

in the dynamics of the infected subjects I, the expression of the Jacobian for the present case is the same as for (1) except for the third row depending on f_3, in which the elements in (82) must be considered. What is then obtained is

$$\frac{\partial f_1}{\partial S_1} = -d - \frac{c\beta I}{N_c} + \frac{c\beta S_1 I}{N_c^2}, \qquad \frac{\partial f_1}{\partial S_2} = \gamma + \frac{c\beta S_1 I}{N_c^2} \tag{83}$$

$$\frac{\partial f_1}{\partial I} = -\frac{c\beta S_1}{N_c} + \frac{c\beta S_1 I}{N_c^2}, \qquad \frac{\partial f_2}{\partial S_2} = -(\gamma + d) \tag{84}$$

$$\frac{\partial f_4}{\partial I} = \varepsilon\delta, \qquad \frac{\partial f_4}{\partial P} = -(\alpha_1 + d) \tag{85}$$

$$\frac{\partial f_5}{\partial I} = (1-\varepsilon)\delta, \qquad \frac{\partial f_5}{\partial P} = \alpha_1, \qquad \frac{\partial f_5}{\partial A} = -(\alpha + d) \tag{86}$$

as for the isolated case, while for the third row one has

$$\frac{\partial f_3}{\partial S_1} = \frac{c\beta I}{N_c} - \frac{c\beta S_1 I}{N_c^2} + \frac{(m_3+n_3)(P+A)}{N^2} \tag{87}$$

$$\frac{\partial f_3}{\partial S_2} = -\frac{c\beta S_1 I}{N_c^2} + \frac{(m_3+n_3)(P+A)}{N^2} \tag{88}$$

$$\frac{\partial f_3}{\partial I} = -(d+\delta) + \frac{c\beta S_1}{N_c} - \frac{c\beta S_1 I}{N_c^2} + \frac{(m_3+n_3)(P+A)}{N^2} \tag{89}$$

$$\frac{\partial f_3}{\partial P} = -\frac{(m_3+n_3)(S_1+S_2+I)}{N^2} \tag{90}$$

$$\frac{\partial f_3}{\partial A} = -\frac{(m_3+n_3)(S_1+S_2+I)}{N^2} \tag{91}$$

The corresponding Jacobian matrix is computed for each of the admissible equilibrium points obtained in the previous Subsection 6.1. Then, for the case $n_3 = 0$, only one solution is considered, whose value changes with m_3, the one in Figure 19. For each value of m_3, one equilibrium point is obtained as well as one corresponding Jacobian matrix. For each of them the five eigenvalues are computed and they are plotted in Figure 24. It can be noted that all the five eigenvalues, three real and one conjugate complex couple, have their real part negative until $m_3 = 2.285\,10^4$, marked with the dotted vertical line. After that value, one eigenvalue becomes positive and the local stability is lost.

The same computations are performed for the two admissible equilibrium points reported in Figures 21 and 22. The eigenvalues of the Jacobian matrix which locally approximates the non linear dynamics in a neighbourhood of the n_3 dependent first equilibrium point are reported in Figure 25, where it is possible to see that for the range considered for n_3, one root is always positive and then the equilibrium point is unstable. On the contrary, for the second equilibrium point, the one in Figure 22, the situation is equivalent to the case of Figure 24: three real eigenvalues and one conjugate complex couple, whose real parts are depicted in Figure 26, solid for the real roots, dashed for the complex ones. They are all negative for $n_3 < 8.4\,10^5$, so yielding to local asymptotic stability of the equilibrium points; for values $n_3 > 8.4\,10^5$ stability condition is no more satisfied.

7. The effects of migration parameters on the individuals evolutions

This Section is devoted to report some behaviour of the system for different values of the coefficients m_1, n_1, m_3 and n_3, according to the stability results discussed in Section 6. The numerical values of the system parameters are, obviously, the ones in Table (1); the initial conditions for all the simulations have been chosen as $S_1(0) = 92000$, $I(0) = 8000$, $S_2(0) = P(0) = A(0) = 0$, aiming at modelling a population in which, initially, the epidemic is not known but some infected individuals are already present.

The first case reported refers to the time evolution of the system where m_1 varies while $n_1 = m_3 = n_3 = 0$. The results are reported in Figures 27–31.

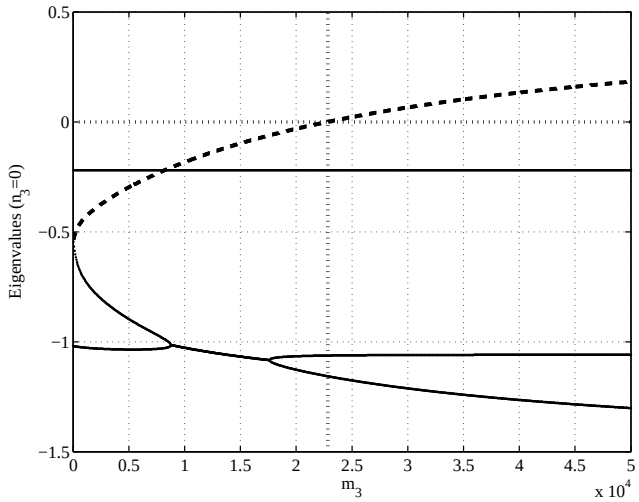

Figure 24: Real part of the five eigenvalues of the Jacobian matrix computed in the first solution for $n_3 = 0$ and $m_3 \in [0, 5\,10^4]$. The dotted line denotes the real part of a couple of conjugate complex roots

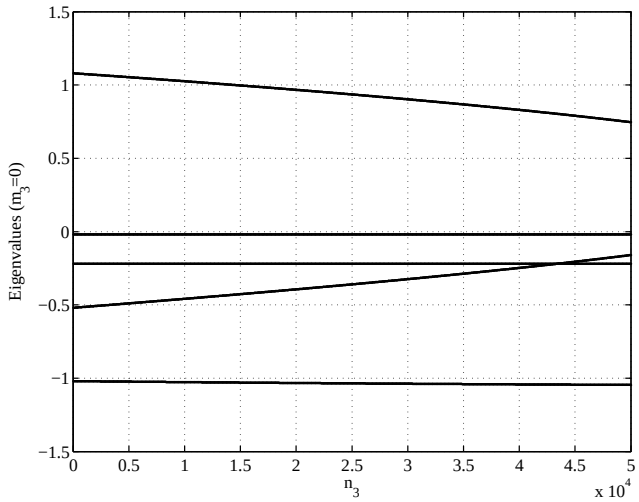

Figure 25: Real part of the five eigenvalues of the Jacobian matrix computed in the first solution for $m_3 = 0$ and $n_3 \in [0, 5\,10^4]$.

In particular, Figure 27 depicts the evolution of the number of unwise healthy population $S_1(t)$ when m_1 changes and Figure 28 reports the same cases for m_1, starting from zero (corresponding to the dashed lines) and increasing its value. The evolution of $S_2(t)$ is not reported because for the initial condition chosen it is constant and equal to zero. Also the time histories of $P(t)$ and $A(t)$

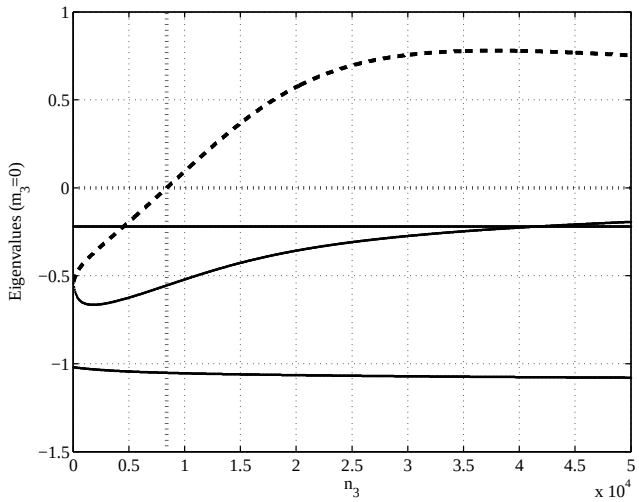

Figure 26: Real part of the five eigenvalues of the Jacobian matrix computed in the second solution for $n_3 = 0$ and $m_3 \in [0, 5\,10^4]$. The dotted line denotes the real part of a couple of conjugate complex roots

are omitted since they have the same shape of $I(t)$. The obvious result that can be evidenced from Figure 27 is that the number of healthy people increases as m_1 grows; unfortunately, this increment makes the infected individuals $I(t)$ grow too. However, a very interesting behaviour of the system can be observed once the evolution of the fraction of diagnosed infected patients $P(t) + A(t)$ w.r.t. the total population is determined, varying m_1, as reported in Figure 29. From these plots it can be seen that, under the hypothesis of an immigration of healthy people driven by the health of the total population, the different values of m_1 affects the transient behaviour only, reaching, for all the m_1, the same steady state value. The same result can be observed in Figure 30, where the fraction of the healthy population $S_1(t) + S_2(t)$ w.r.t. the total one is reported: also in this case, the steady state value is the same. Then, it is possible to conclude that, for the model considered, an immigration of healthy individuals makes the population grow, as evidenced in Figure 31, each of the classes grow (Figures 27 and 28) but the fraction of healthy population as well as the fraction of infected one tends to remain unchanged even if the rate of immigration (m_1) increases.

In Figures 32–36 the results of simulations for different values of n_1 while $m_1 = m_3 = n_3 = 0$ are reported. This represents an emigration of healthy people based on the presence of infection in the population. As expected, both $S_1(t)$ and $I(t)$ decrease, as reported in Figure 32 and 33 respectively, $I(t)$ more sensibly than $S_1(t)$. However, also in this case the percentage of infected subjects, plotted in Figure 34 and the one of healthy individuals, depicted in Figure 35, tends to be unchanged as n_1 changes, having the same steady state values. Differently form the case of variation of m_1, in this case the transients present

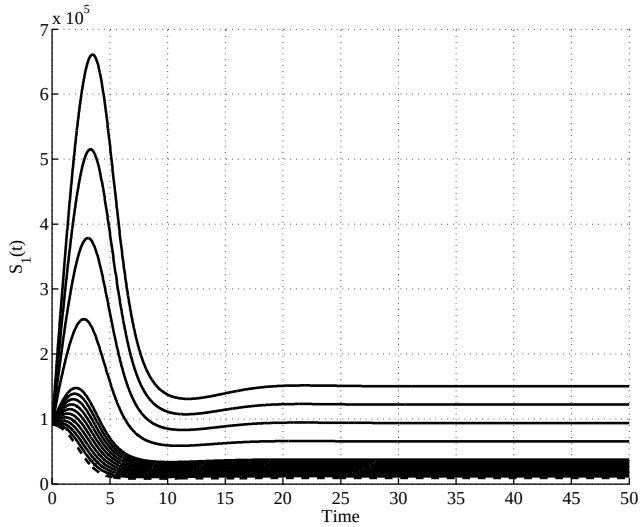

Figure 27: Time history of $S_1(t)$ for different values of m_1. The dotted line corresponds to $m_1 = 0$; values increases according to m_1

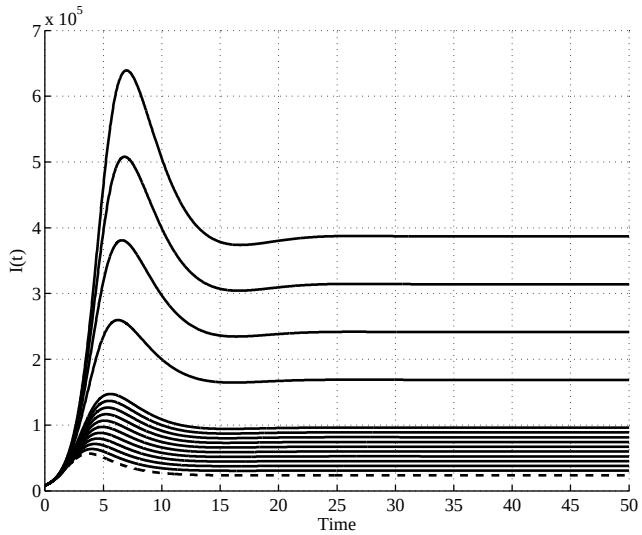

Figure 28: Time history of $I(t)$ for different values of m_1. The dotted line corresponds to $m_1 = 0$; values increases according to m_1

a higher amplitudes as n_1 increases. This result can be used to better understand the actual dangerousness of the phenomenon, since high values of relative infected individuals can be limited to finite time intervals, during the transient, and may not represent a real social alarm situation. Figure 36 shows that in

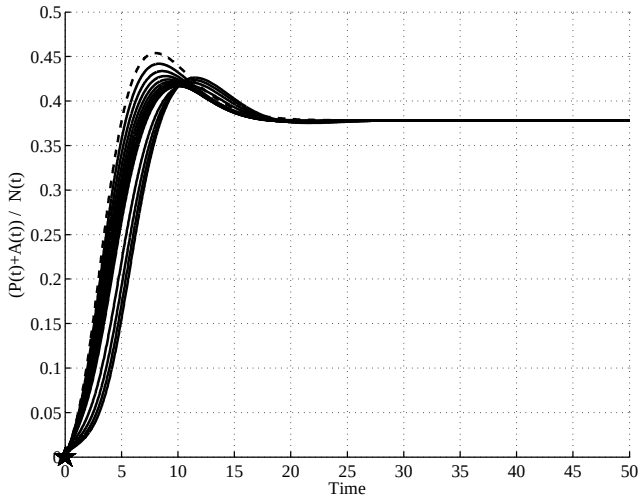

Figure 29: Time evolution of the relative number of diagnosed patients $P(t) + A(t)$ w.r.t. the total population for different values of m_1. The dotted line corresponds to $m_1 = 0$

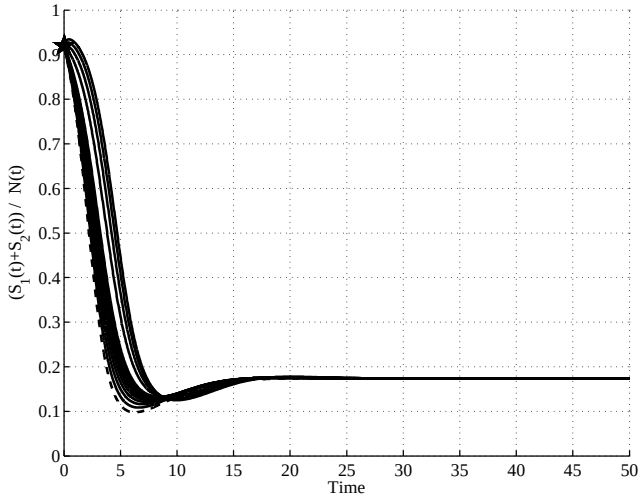

Figure 30: Time evolution of the relative number of healthy individuals $S_1(t) + S_2(t)$ w.r.t. the total population, for different values of m_1. The dotted line corresponds to $m_1 = 0$

this case the total population decreases as the emigration rate increases, but with oscillations during the transient with increasing amplitude.

A second set of numerical simulations addresses the case of migration which affects the infected population $I(t)$; in this case, the couple of coefficients m_1 and n_1 are always fixed to zero. The results are reported in the next Figures 37–46, where the evolution of the system is depicted for different values of m_3,

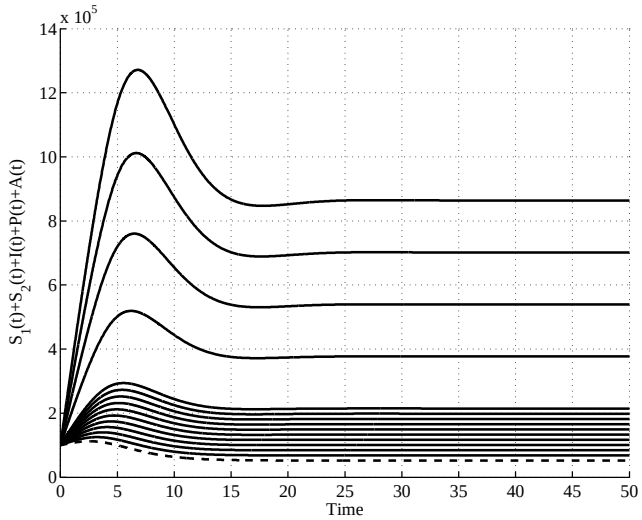

Figure 31: Time evolution of the population for different values of m_1. The dotted line corresponds to $m_1 = 0$

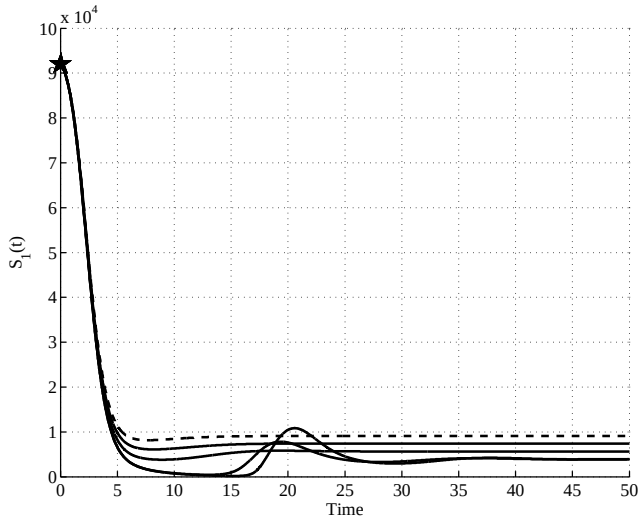

Figure 32: Time history of $S_1(t)$ for different values of n_1. The dotted line corresponds to $n_1 = 0$

while $n_3 = 0$, modelling a flux of immigrants from outside the group, and then for different values of n_3 with $m_3 = 0$, representing an emigration phenomenon.

In Figure 37 the time history of the healthy individuals $S_1(t)$ is plotted for different values of m_3 while Figure 38 reports the same situation for the infected subjects $I(t)$. Their behaviours are compatible with what can be expected: the

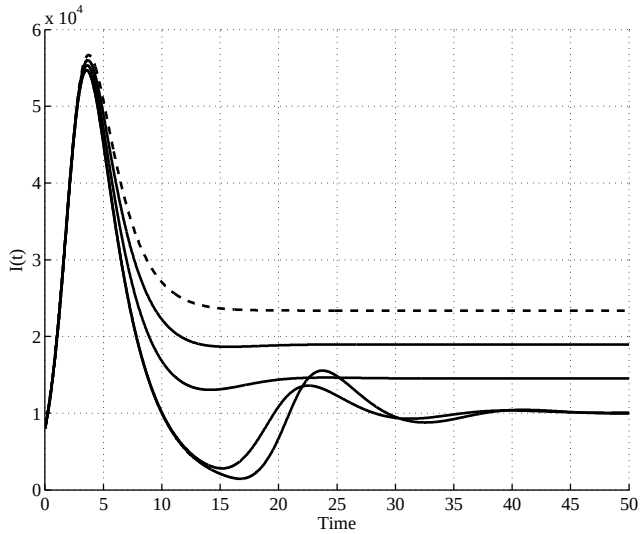

Figure 33: Time history of $I(t)$ for different values of n_1. The dotted line corresponds to $n_1 = 0$

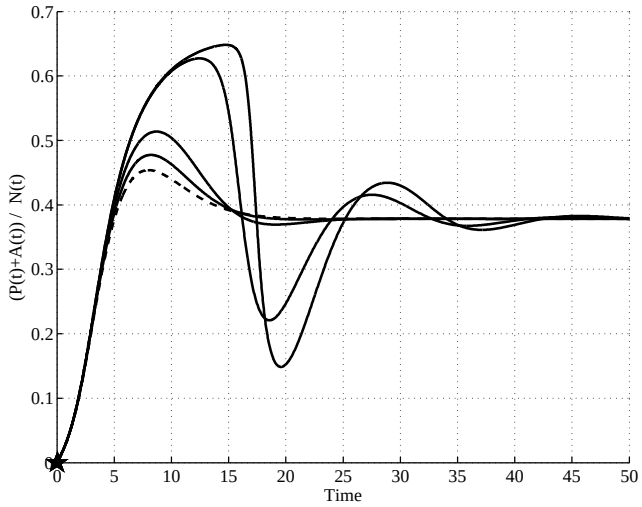

Figure 34: Time evolution of the relative number of diagnosed patients $P(t) + A(t)$ w.r.t. the total population, for different values of n_1. The dotted line corresponds to $n_1 = 0$

number of individuals in the class of infected $I(t)$ grows as m_3 increases; at the same time, the uninfected people decrease due to the augmented probability of infection due to the larger $I(t)$ population. However, since the influence of the immigration acts directly on the dynamic of $I(t)$, the growth of $I(t)$ is more accentuated then the decrement of $S_1(t)$, being this latter a secondary effect.

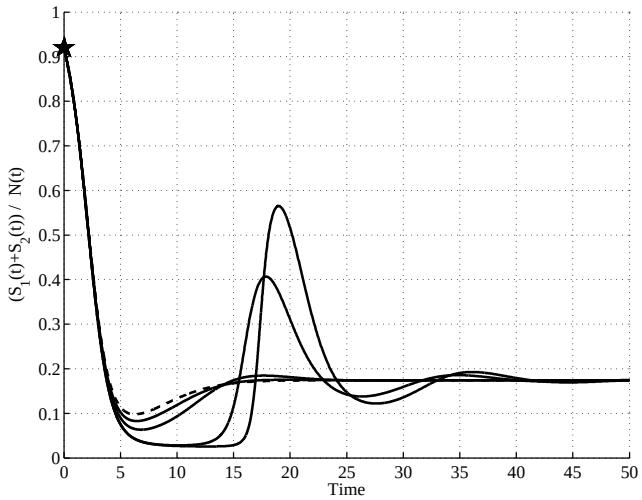

Figure 35: Time evolution of the relative number of healthy individuals $S_1(t) + S_2(t)$ w.r.t. the total population, for different values of n_1. The dotted line corresponds to $n_1 = 0$

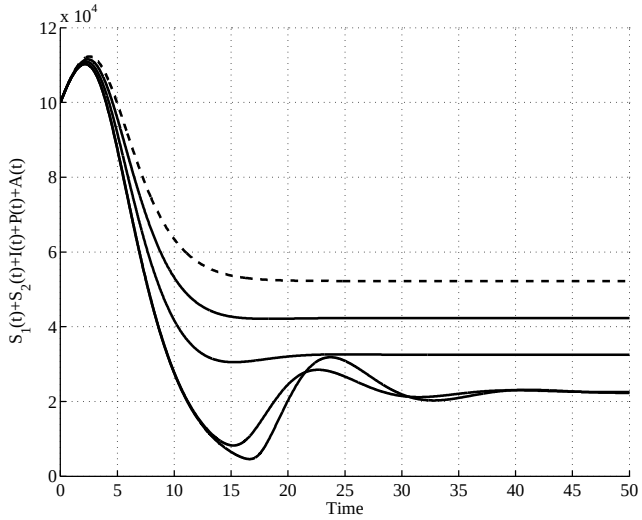

Figure 36: Time evolution of all the population for different values of n_1. The dotted line corresponds to $n_1 = 0$

This characteristic of the system behaviour is confirmed looking at Figures 39 and 40 in which the fraction of infected and healthy population are reported respectively: the first increases while the second decreases. However, these variations have the combined effect of making the total population sensibly increase, as reported in Figure 41, so having a society with higher number of

individuals but composed by an even higher number of infected components.

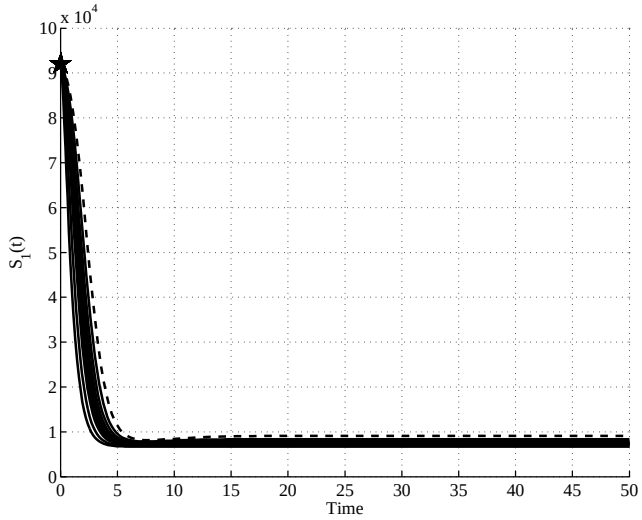

Figure 37: Time history of $S_1(t)$ for different values of m_3. The dotted line corresponds to $m_3 = 0$

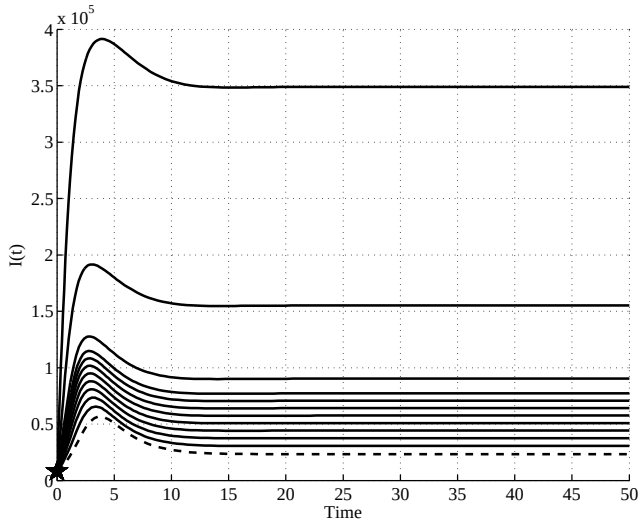

Figure 38: Time history of $I(t)$ for different values of m_3. The dotted line corresponds to $m_3 = 0$

The opposite effect of an emigration from the class of infected $I(t)$, modelled setting $m_3 = 0$ and choosing different values for n_3, can be analysed making use of Figures 42–46. Following the same order as in the the previous cases, the first

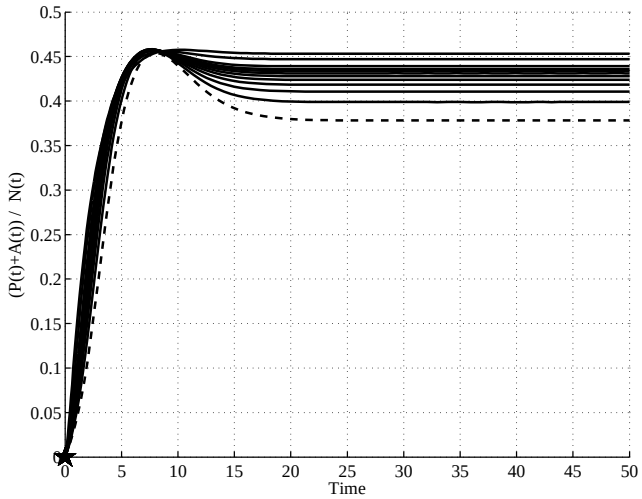

Figure 39: Time evolution of the relative number of diagnosed patients $P(t) + A(t)$ w.r.t. the total population, for different values of m_3. The dotted line corresponds to $m_3 = 0$

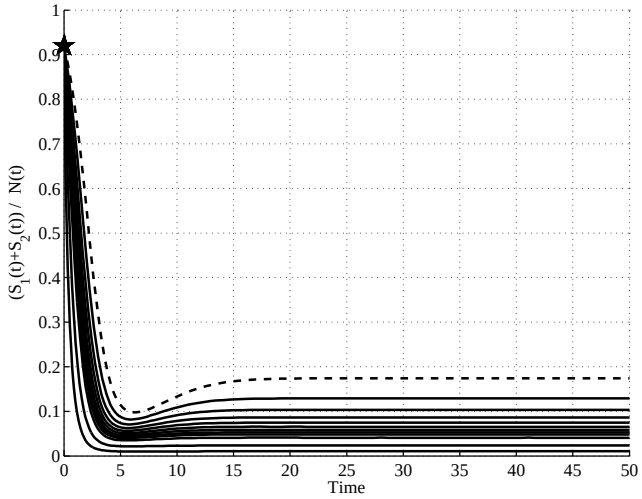

Figure 40: Time evolution of the relative number of healthy individuals $S_1(t) + S_2(t)$ w.r.t. the total population, for different values of m_3. The dotted line corresponds to $m_3 = 0$

two Figures 42 and 43 depict the time history of $S_1(t)$ and $I(t)$ respectively. As expected, the steady state values of the uninfected individuals $S_1(t)$ increases while for the infected $I(t)$ it can be observed a more sensible decrement. The transient, as in the case of emigration from $S_1(t)$, is characterised by a high oscillatory behaviour, in this case more accentuated than in the Figures 32 and 33. In correspondence, the fraction of diagnosed infected people with respect

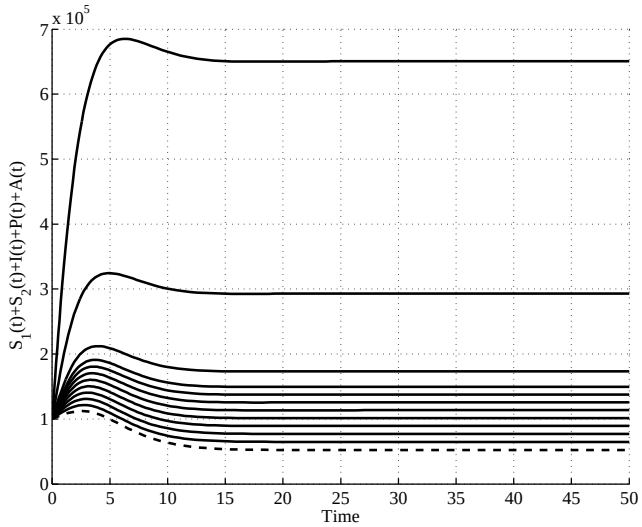

Figure 41: Time evolution of all the population, for different values of m_3. The dotted line corresponds to $m_3 = 0$

to the total population decreases for higher values of n_3 and, contemporary, the relative number of uninfected individuals increases, once their steady state behaviour is observed in Figures 43 and 45. But in the same Figures, the transients show a very large variations of the components. This fact proves the necessity to have a reliable mathematical model to be able to predict some unexpected behaviours or to explain the presence of values in some time intervals that, intuitively, are not obvious. This is well evidenced in Figure 46, in which, without the support of a model, it is not easy to justify the large variations of the total population as the time passes.

8. Discussion of the results

A final discussion on the results presented in the previous Sections, with particular reference to Sections 5 and 7, is here shortly reported. The approach followed in the present work aims to put in evidence the effects of incoming and/or out-coming migrations, when they involve health individuals which do not put a great attention to the modalities of virus spread or infected persons not aware of being ill and contagious.

Among the goals of such an analysis there is the possibility of previewing and understanding the characteristics of the behaviours of some classes of individuals under particular external contributions.

The main aspects that can be evidenced once the numerical results are compared and interpreted are

i. an immigration involving healthy individuals not well informed on the risks of unwise behaviours produces an increment of people in all the

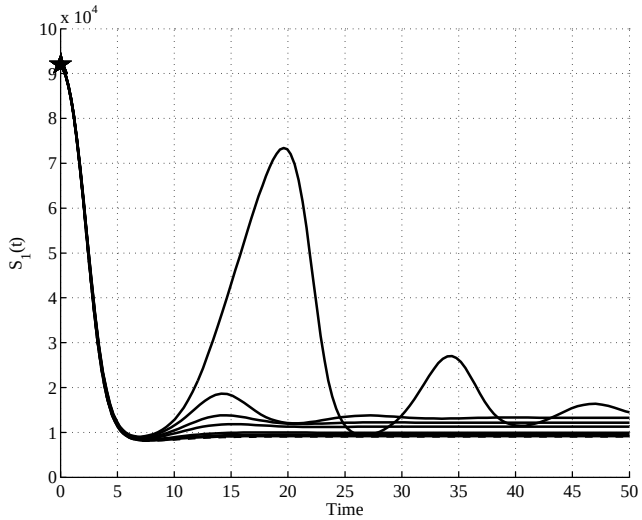

Figure 42: Time history of $S_1(t)$ for different values of n_3. The dotted line corresponds to $n_3 = 0$

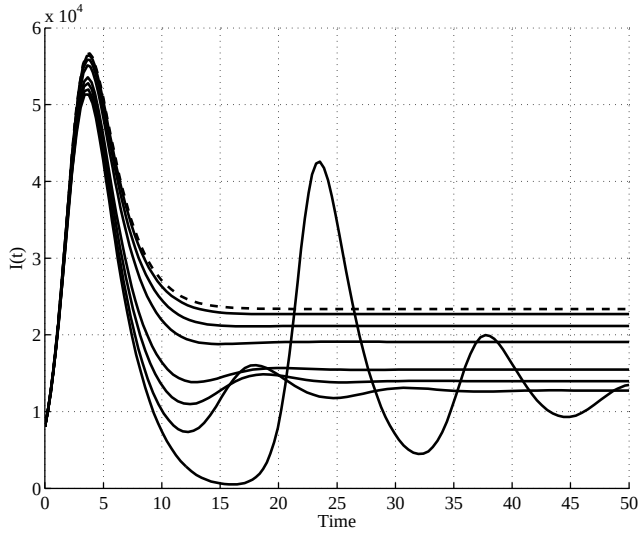

Figure 43: Time history of $I(t)$ for different values of n_3. The dotted line corresponds to $n_3 = 0$

classes of the population, since the interactions producing virus transmission increase. However, at steady state, the ratio of health population and the one of infected individuals with respect to the total one is constant;

ii. emigration involving the same population as in i. implies an evolution

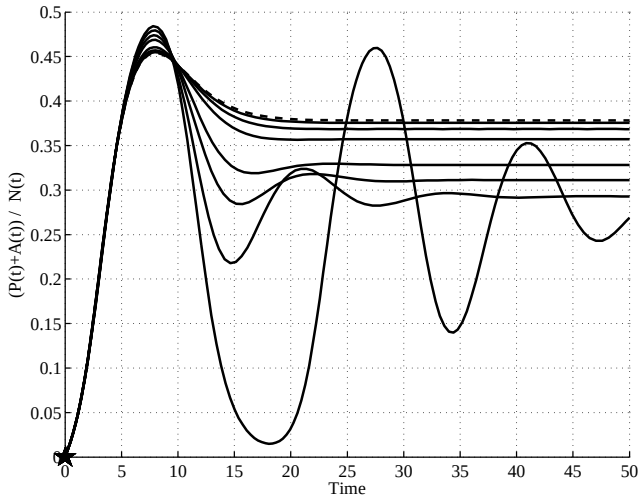

Figure 44: Time evolution of the relative number of diagnosed patients $P(t) + A(t)$ w.r.t. the total population, for different values of n_3. The dotted line corresponds to $n_3 = 0$

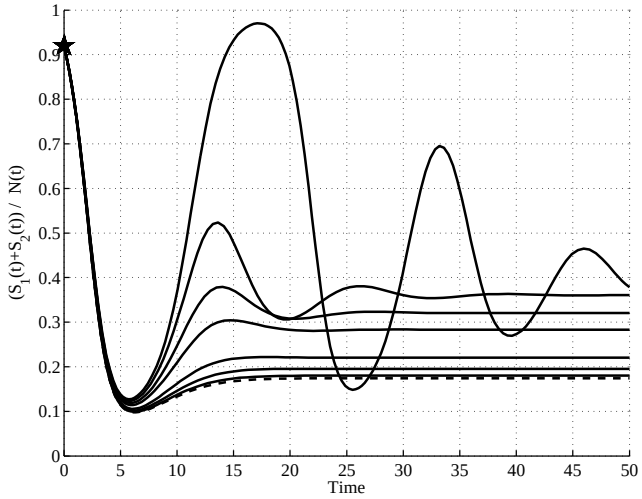

Figure 45: Time evolution of the relative number of healthy individuals $S_1(t) + S_2(t)$ w.r.t. the total population, for different values of n_3. The dotted line corresponds to $n_3 = 0$

opposite to the previous one, with a decrement of people in all classes, going, at steady state, again to constant ratios, but with the presence of oscillations in the transient. This peculiar behaviour is interesting to be stressed since there are time intervals with increment of individuals, healthy and infected, despite the emigration phenomena. This fact does not characterises the behaviour of the dynamics when the vaccination,

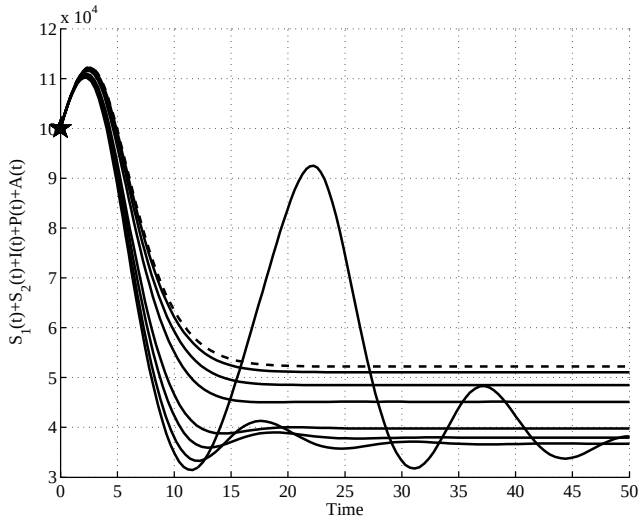

Figure 46: Time evolution of all the population for different values of n_3. The dotted line corresponds to $n_3 = 0$

which acts on the same subjects, is applied;

iii. when the immigration involves infected people unconscious of their status, the effect is the expected one: the number of healthy people decreases while all the infected ones increase. This produces an increment of the total population, but it is due to a higher number of infected individuals;

iv. the emigration among people of the same class as in *iii.* at steady state shows the opposite behaviour with respect to the previous case, as expected. However, the transient is characterised by an oscillatory behaviour, as in the case *ii.*; this fact implies that a correct interpretation of the population dynamics cannot be correctly performed over short time period only.

9. Conclusions and future developments

In this chapter, the study of the effects of the interactions among different groups is performed by modelling the whole population as the aggregate of each one and introducing terms in the dynamics which take into account the possible interconnections. These results are obtained starting from the analysis developed for the single group dynamics modeling each interaction as additional inputs and/or changes in the parameter values.Such effects can be modelled as constant fluxes, which introduce additive constant terms in the dynamics, or can be supposed driven by some characteristic of the group behaviour, such as a *higher* or *lower* level of healthy, for example. As case study, the epidemic spread considered is the HIV-AIDS one, assuming a new model in which the

classical scheme that includes susceptible people and three classes of infected ones (infected not aware of their status, patients in the pre-Aids and in the AIDS conditions) is enriched by splitting the class of susceptible individuals into those aware of the risks of this virus and those that adopt irresponsible acts. The proposed analysis, particularly suitable in describing, for the chosen model, the migration phenomena, is useful to predict unexpected behaviours especially in the transient period in which oscillatory behaviours for the classes of infected patients, as evidenced in the discussion.

Since all the results presented are highly dependent on the model structure and parameters values, future developments should involve real data analysis and model validation. Moreover, the explicit introduction of the detailed interactions between more than one population is mandatory for putting in evidence the migration fluxes. This is preparatory for the introduction of a control strategy for reducing the virus spread between populations despite the globalization needs.

References

Behncke, H., 2000. Optimal control of deterministic epidemics. Optimal control applications and methods 21 (2), 269–285.

Casagrandi, R., Bolzoni, L., Levin, S., Andreasen, V., 2006. The sirc model and influenza. A. Mathematical Biosciences 200 (2), 152–169.

Chalub, F., Souza, M., 2011. The sir epidemic model from a pde point of view. Mathematical and computer modeling 58, 1568–1574.

Chang, H., Astolfi, A., 2009. Control of hiv infection dynamics. IEEE Control Systems 213 (2), 28–39.

Crush, J., Williams, B., Gouws, E., Lurie, M., 2005. Migration and hiv/aids in south africa. Development Southern Africa 22 (3), 293–317.

Dadlani, A., Kumar, M., Murugan, S., Kim, K., 2014. System dynamics of a refined epidemic model for infection propagation over complex networks. IEEE Systems Journal 10 (4), 1316–1325.

Di Giamberardino, P., Compagnucci, L., Giorgi, C. D., Iacoviello, D., 2018. Modeling the effects of prevention and early diagnosis on hiv/aids infection diffusion. IEEE Transactions on Systems, Man and Cybernetics: Systems, in press.

Di Giamberardino, P., Iacoviello, D., 2017a. Optimal control of SIR epidemic model with state dependent switching cost index. Biomedical Signal Processing and Control 31 (2), 377–380.

Di Giamberardino, P., Iacoviello, D., 2017b. An optimal control problem formulation for a state dependent resource allocation strategy. In Proceedings

of the 14th International Conference on Informatics in Control, Automation and Robotics 1, 186–195.

Di Giamberardino, P., Iacoviello, D., 2018. Lq control design for the containment of the hiv/aids diffusion. Control Engineering Practice 77, 162–173.

Iacoviello, D., Liuzzi, G., 2008a. Fixed/free final time sir epidemic models with multiple controls. International Journal of Simulation and Modelling 7 (2), 81–92.

Iacoviello, D., Liuzzi, G., 2008b. Optimal control for sir epidemic model: a two treatments strategy. in Proc. of IEEE 16th Mediterranean Conference on Control and Automation 7 (2), 81–92.

Iacoviello, D., Stasio, N., 2013. Optimal control for sirc epidemic outbreak. Computer Methods and Programs in Biomedicine 110 (3), 333–342.

Joshi, H., 2002. Optimal control of an hiv immunology model. Optimal control applications and methods 23 (2), 199–213.

Jr, J. C., Hoever, G., Morgenstern, B., Preiser, W., Vogel, J., Hofmann, W., Bauer, G., Michaelis, M., Rabenau, H., Doerr, H., 2004. Infection of cultured intestinal epithelial cells with severe acute respiratory syndrome coronavirus. CMLS, Cell. Mol. Life Sci. 61 (16), 2010–2012.

Kryftis, Y., Mastorakis, G., Mavromoustakis, C., Batalla, J., Rodrigues, J., Dobre, C., 2017. Resource usage prediction models for optimal multimedia content provision. IEEE Systems Journal 11 (4), 2852–2863.

Kuniya, T., Nakata, Y., 2012. Permanence and extinction for a nonautonomous seirs epidemic model. Applied Mathematics and Computation 218 (2), 9321–9331.

Mascio, M., Ribeiro, R., Markowitz, M., Ho, D., , Perelson, A., 2004. Modeling the long-term control of viremia in hiv-1 infected patients treated with antiretroviral therapy. Math. Biosci. 188 (25), 47–62.

Nagelkerke, N., Jha, P., de Vlas, S., Korenromp, E., Moses, S., Blanchard, J., Plummer, F., 2002. Modelling hiv/aids epidemics in botswana and india: impact of interventions to prevent transmission. Bull World Health Organ. 80 (2), 89–96.

Naresh, R., Tripathi, A., Sharma, D., 2009. Modeling and analysis of the spread of aids epidemic with immigration of hiv infectives. Mathematical and Computer Modelling 49 (25), 880–892.

Nowzari, C., Preciado, V. M., Pappas, G. J., 2016. Analysis and control of epidemics. a survey of spreading processes on complex networks. IEEE Control Systems Magazine 80 (2), 24–26.

Pinto, C., Rocha, D., 2012. A new mathematical model for co-infection of malaria and hiv. 4th IEEE International Conference on Nolinear Science and Complexity 49 (25), 33–39.

Tanaka, G., Urabe, C., 2014. Random and targeted interventions for epidemic control in metapopulation models. SCIENTIFIC REPORTS 4:5522 4 (2), 1–8.

Wodarz, D., 2001. Helper-dependent vs. helper-independent ctl responses in hiv infection: Implications for drug therapy and resistance. Journal theor. Biol. 213 (2), 447–459.

Wodarz, D., Nowak, M., 1999. Specific therapy regimes could lead to long-term immunological control of hiv. Proc. Nat. Acad. Sci. 96 (25), 14464–14469.

X.Yan, Y.Zou, 2008. Optimal and sub-optimal quarantine and isolation control in sars epidemics. Mathematical and computer modelling 47 (2), 235–245.

Zhou, Y., Yang, K., Zhou, K., Wang, C., 2014. Optimal treatment strategies for hiv with antibody response. Journal of applied mathematics 52 (2), 1–13.